Available online at www.sciencedirect.com

ScienceDirect

Geochimica et Cosmochimica Acta 121 (2013) 374–397

Geochimica et Cosmochimica Acta

www.elsevier.com/locate/gca

Mg-isotopic fractionation in the manila clam (*Ruditapes philippinarum*): New insights into Mg incorporation pathway and calcification process of bivalves

Frédéric Planchon [a,b,c,*], Céline Poulain [b], Denis Langlet [b,c], Yves-Marie Paulet [a,b], Luc André [c]

[a] *Université Européenne de Bretagne, Brest, France*
[b] *Laboratoire des Sciences de l'Environnement Marin (LEMAR), CNRS, IRD, UMR 6539, IUEM, Technopôle Brest Iroise, Place Nicolas Copernic, F-29280 Plouzané, France*
[c] *Department of Geology, Section of Mineralogy and Petrography, Royal Museum for Central Africa, Leuvensesteenweg 13, B-3080 Tervuren, Belgium*

Received 8 March 2012; accepted in revised form 1 July 2013; available online 13 July 2013

Abstract

We estimate the magnesium stable isotopic composition ($\delta^{26}Mg$) of the major compartments involved in the biomineralisation process of euryhaline bivalve, the manila clam *Ruditapes philippinarum*. Our aim is to identify the fractionation processes associated with Mg uptake and its cycling/transport in the bivalve organism, in order to better assess the controlling factors of the Mg isotopic records in bivalve shells. $\delta^{26}Mg$ were determined in seawater, in hemolymph, extrapallial fluid (EPF), soft tissues and aragonitic shell of adult clams collected along the Auray River estuary (Gulf of Morbihan, France) at two sites showing contrasted salinity regimes. The large overall $\delta^{26}Mg$ variations (4.16‰) demonstrate that significant mass-dependent Mg isotopic fractionations occur during Mg transfer from seawater to the aragonitic shell.

Soft tissues span a range of fractionation factors relative to seawater ($\Delta^{26}Mg_{soft\ tissue\text{-}seawater}$) of 0.42 ± 0.12‰ to 0.76 ± 0.12‰, and show evidence for biological isotopic fractionation of Mg. Hemolymph and EPF are on average isotopically close to seawater ($\Delta^{26}Mg_{hemolymph\text{-}seawater} = -0.20 \pm 0.27$‰; 2 sd; $n = 5$ and $\Delta^{26}Mg_{EPF\text{-}seawater} = -0.23 \pm 0.25$‰; 2 sd; $n = 5$) indicating (1) a predominant seawater origin for Mg in the intercellular medium and (2) a relatively passive transfer route through the bivalve organism into the calcifying fluid. The lightest isotopic composition is found in shell, with $\delta^{26}Mg$ ranging from -1.89 ± 0.07‰ to -4.22 ± 0.06‰. This range is the largest in the dataset and is proposed to result from a combination of abiotic and biologically-driven fractionation processes. Abiotic control includes fractionation during precipitation of aragonite and accounts for $\Delta^{26}Mg_{aragonite\text{-}seawater} \approx 1000 \ln \alpha_{aragonite\text{-}seawater} = -1.13 \pm 0.28$‰ at 20 °C based on literature data. Deviations from inorganic precipitate (expressed as $\Delta^{26}Mg_{Physiol}$) appear particularly variable in the clam shell, ranging from 0.03‰ to −2.20‰, which indicates that bivalve shell formation can proceed either under fractionation similar to inorganically-precipitated aragonite or under variable physiological influences. These physiological isotopic effects may be consistent with a regulation of dissolved Mg content in hemolymph and/or EPF due to Mg incorporation into soft tissue and/or Mg fixation by organic macromolecules. Using closed- and open-system models we estimate that $\Delta^{26}Mg_{Physiol}$ can be satisfactorily resolved with a remaining Mg fraction in hemolymph and/or EPF of 74% down to 2%. However, this feature is not reflected in our hemolymph and EPF data and may indicate that regulation processes and isotopic fractionation may take place in self-contained spaces located close to calcification sites. The potential role of the shell organic matrix, which may host non-lattice-bound Mg in the shell, is also discussed but remains difficult to assess with our data.

* Corresponding author at: Université Européenne de Bretagne, Brest, France. Tel.: +33 (0) 2 98 49 86 98; fax: +33 (0) 2 98 49 86 45.
E-mail address: frederic.planchon@univ-brest.fr (F. Planchon).

0016-7037/$ - see front matter
http://dx.doi.org/10.1016/j.gca.2013.07.002

Regarding the large physiological effects, the $\delta^{26}Mg$ record in the Manila clam shell offers limited potential as a proxy of temperature or seawater Mg isotopic composition. In contrast, the sensitivity of its $\delta^{26}Mg$ to the salinity regime may offer an interesting tool to track changes in clam biological activity in estuarine environments.

1. INTRODUCTION

Skeletal remains of marine calcifying organisms have long been recognised as valuable archives of physical and chemical processes in the world's oceans. Major climatic and biogeochemical parameters, such as oceanic temperature, salinity, alkalinity, pH, water dynamics or productivity, can be inferred from the isotopic and elemental composition of corals, sclerosponges, foraminifers, coccoliths and echinoderms (e.g. Gagan et al., 2000; Henderson, 2002; Immenhauser et al., 2005; Rosenheim et al., 2005b; Hippler et al., 2006; Ourbak et al., 2006; Grottoli and Eakin, 2007; Wombacher et al., 2011). During the last decade, calcified tissues of bivalve mollusks have been increasingly used to reconstruct seasonal to multi-decadal paleoclimatic and paleoenvironmental variability from extratropical oceans to coastal marine settings (Klein et al., 1996a; Wanamaker et al., 2008; Schöne and Gillikin, 2013).

Underlying the use of stable and radiogenic isotopes and element-to-calcium ratios as proxies is the assumption that skeletal chemistry reflects a particular environmental variable that is not significantly influenced by organism physiology or other external factors. Nevertheless, it is now clear that conventional proxies can often react to more than one environmental parameter and also be affected by taxon- and species-specific biological processes, which potentially limit their archival potential (e.g. Adkins et al., 2003; Geist et al., 2005; Gillikin et al., 2005, 2006; Carré et al., 2006; Sinclair and Risk, 2006; Takesue et al., 2008). This is especially true for bivalves for which increasing number of studies demonstrate that, at least for Mg, biological controls can strongly affect the shell composition (e.g. Klein et al., 1996a; Vander Putten et al., 2000; Lazareth et al., 2003, 2007; Takesue and van Geen, 2004; Foster et al., 2008; Freitas et al., 2008). Whereas paleoclimatic studies can circumvent these problems by drawing on robust proxy calibration and validation for target organisms, understanding the chemical and physiological mechanisms behind so-called "vital effects" (Urey et al., 1951) remains a challenge. A deeper understanding of vital effects can be gained by developing new descriptive parameters for the biocalcification process.

New proxy-based approaches include non-traditional stable isotope geochemistry of alkaline and alkaline earth elements that have emerged in the last decade. In this regard, and owing to recent achievements in multiple-collector inductively coupled plasma mass spectrometry (MC-ICP-MS) (Galy et al., 2001), precise and accurate Mg isotopic ratios are now accessible for most environmental matrices, including biogenic carbonates (Chang et al., 2003, 2004; de Villiers et al., 2005; Pogge von Strandmann, 2008; Hippler et al., 2009; Ra et al., 2010; Wombacher et al., 2011). Resolving Mg isotope fractionation in biologically precipitated shells and skeletons offers twofold interest: as a new, independent proxy of oceanographic process and as a tool to better describe the complex internal cycling of Mg during the biocalcification process.

Recent studies have shown that biominerals secreted by corals, coccoliths, foraminifers, bivalves, echinoids, scaphopods, brachiopods and coralline red algae define a wide array of Mg isotopic ratios (Chang et al., 2004; Pogge von Strandmann, 2008; Hippler et al., 2009; Ra et al., 2010; Müller et al., 2011; Wombacher et al., 2011; Yoshimura et al., 2011). The large isotopic fractionation of Mg is ascribed to both abiotic and biological mechanisms. It includes carbonate precipitation with variable fractionation factor according to crystal structure – the calcite polymorph showing a lighter signature compared to an aragonitic one – combined with species-specific physiological controls (Pogge von Strandmann, 2008; Hippler et al., 2009; Müller et al., 2011; Wombacher et al., 2011). Mg isotope fractionation into calcitic corals, sclerosponges and coralline red algae compare favourably to inorganic calcite precipitation deduced from speleothems (Galy et al., 2002) and suggest weak or negligible physiological influence. Conversely, coccoliths, foraminifers, bivalves, echinoids and brachiopods exhibit diverse levels of biological controls, with isotopic deviations being towards either lighter (e.g. foraminifera and bivalve) or heavier (e.g. coccolith, echinoid, brachiopod) signatures compared to the inorganically-precipitated $CaCO_3$ (Chang et al., 2004; Pogge von Strandmann, 2008; Hippler et al., 2009).

For most of these calcifying species (except bivalves), environmental parameters such as temperature and salinity have been shown to weakly affect Mg isotopic ratios, limiting its usefulness in paleothermometry (Chang et al., 2004; Pogge von Strandmann, 2008; Hippler et al., 2009). Instead, this insensitivity makes corals, foraminifers, echinoids, brachiopods and coralline red algae ideally suited to constraining past variations in the Mg isotope budget of the ocean. It may also help to address key questions about the large-scale geochemical processes that regulate seawater chemistry throughout Earth's history (e.g. dolomitization, continental weathering, hydrothermal activity) (de Villiers et al., 2005; Tipper et al., 2006). Accounting for the strong taxon- and species-specific biological fractionations potentially induced by contemporaneous and fossil marine organisms is a prerequisite for validating this proxy relationship (Pogge von Strandmann, 2008; Hippler et al., 2009; Wombacher et al., 2011).

The magnitude and diversity of biologically driven Mg isotopic partitioning remains poorly understood, although it underlies the presence of different fractionation steps occurring during Mg transport from seawater to skeleton. Indeed, our knowledge of Mg isotope behaviour in biolog-

ical systems is currently restricted to terrestrial plants (Black et al., 2008; Bolou-Bi et al., 2010) and to Mg-bearing specific organic compounds such as chlorophylls (Black et al., 2006, 2008; Ra and Kitagawa, 2007). Such information is clearly needed for marine calcifiers, and is relevant in studying the diversity of physiological controls exerted by these organisms.

Here, we examine Mg isotopic fractionation in a euryhaline bivalve, the manila clam *Ruditapes philippinarum*, a veneridae species that has been naturalized for aquaculture and has colonized most embayments along the French Atlantic Coast since the 1990s. We compare the different internal constituents (extrapallial fluid, hemolymph, and soft tissues) with the aragonitic shell and surrounding seawater. We specifically investigate whether uptake and transport mechanisms in the bivalve body produce a measurable fractionation, and how this process explains the shell's Mg isotopic ratios, considering both the prismatic and nacreous layers, and whether different salinity regimes along an estuary influence shell signatures. This approach complements a recent study (Hippler et al., 2009) performed on another bivalve, *Mytilus edulis*, for which biological factors were shown to play a key role in the Mg isotopic composition of the calcitic shell. That study, however, was unable to arrive at a mechanistic explanation of this fractionation.

2. MATERIALS AND METHODS

2.1. Sampling and specimen preparation

The manila clam *R. philippinarum* lives buried, a few centimeters deep, in muddy and sandy sediments of both intertidal and subtidal zones. It inhabits the mouths of estuaries in which salinities range from 16 to 36 psu, with an optimum between 20 and 26 psu (Nie, 1991). Because of its importance for aquaculture and fisheries this species is well studied in terms of its biology and physiology (e.g. Richardson, 1987; Goulletquer et al., 1989; Kim et al., 2001; Flye-Sainte-Marie et al., 2009).

Two sampling sites were considered, both located within the Auray River estuary in the Gulf of Morbihan (Southern Brittany, France, Fig. 1). The first site, Locmariaquer (Loc), is a coastal marine setting close to the mouth of the gulf where salinity is relatively stable, varying from 27 to 35 psu on a monthly and seasonal time scale. The second site, Le Bono, is located approximately 9 km upstream in the subtidal zone of the Auray River estuary. The Le Bono site exhibits brackish water conditions, with salinity ranging from 3 to 33 psu on a semidiurnal tidal cycle (mean tidal range of about 4–5 m). Depth, salinity and temperature were recorded every 10 min using an autonomous data logger (YSI 600-OMS) and detailed data can be found elsewhere (Poulain et al., 2011). In April 2007, adult (four to 6 year-old) manila clams *R. philippinarum* were collected by diving at high tide in the subtidal zone; one specimen (length 47 mm) was sampled at Locmariaquer and four (average length 49 mm; $1\sigma = 2$ mm) at Le Bono.

Immediately after collection, the internal fluids (extrapallial fluid and hemolymph) of each living specimen were sampled using syringes equipped with sterile needles. Localization of hemolymph and EPF in the bivalve's body is illustrated in Fig. 2. Between 100 and 200 µL of extrapallial fluid (EPF) and hemolymph were retrieved in pre-cleaned vials and stored at 4 °C. Also at each site, duplicate 30 mL seawater samples were collected at high tide in acid-cleaned High-Density Polyethylene (HDPE) bottles, filtered at 0.45 µm onboard, acidified at 1% with double-distilled HNO_3 and stored at 4 °C.

At the laboratory, the soft tissues were removed from the shells and then dissected in Milli-Q water to separate the mantle and adductor muscle from remaining organs such as the gill, digestive system, heart and palps. These three distinct fractions (i.e. mantle, muscle and remaining organs) were separately rinsed with Milli-Q water to remove sediment particles, lyophilized, powdered and homogenized before acid digestion. Mixed acid and oxidative attack was performed in PFA Savillex on ~50 mg of sample powder with 2 mL of double-distilled concentrated HNO_3 and 2 mL of H_2O_2 at 70 °C. After total dissolution (1 day), solutions were evaporated to dryness, re-dissolved with 25 mL of 5% (v/v) double-distilled HNO_3 solution and stored in 30 mL acid-cleaned HDPE bottles at 4 °C. The internal fluids were centrifuged to eliminate organic particulate matter and supernatant was recovered in 2 mL pre-cleaned vials and stored at 4 °C. To determine Mg, Ca, Na and K concentrations (Table 1), aliquots of filtered seawater, internal fluids, and dissolved soft tissue samples were analyzed by Inductively Coupled Plasma Mass Spectrometry (SF-ICP-MS, Element 2). For the soft tissue, Al/Mg and Si/Mg ratios were also determined to confirm removal of Mg-rich clay material. The mantle, muscle and remaining organs had Al/Mg and Si/Mg ratios of <0.05 g/g, indicating an efficient cleaning procedure.

After soft-tissue removal, the equivalve shells of *R. philippinarum* were cleaned with repeated rinsing and ultrasonications steps, and finally dried at room temperature. The periostracum surrounding shell (Fig. 2) was first removed from the sampling area using abrasive paper along the ventral margin of the shell. As shown in Fig. 3, the carbonate samples for Mg isotope determination were obtained from two distinct parts: the inner nacreous layer and outer prismatic layer, using an acid-cleaned scalpel. The outer prismatic layer was sampled at the ventral margin over a distance of ~1 mm along the maximal growth axis; for some specimens, a consecutive ~1 mm thick sample was taken. For the single specimen of Locmariaquer, the two valves were considered. The carbonate powders (5–20 mg) were dried, weighed and dissolved in acid-cleaned PFA beakers with 2 mL of 5% (v/v) double-distilled HNO_3 and 2% (v/v) ultra-pure H_2O_2 solution at 80 °C for 6 h. Dissolved samples were then transferred to acid-cleaned HDPE bottles and stored at 4 °C. Mg/Ca and Sr/Ca ratios were determined in aliquots of dissolved carbonate samples by SF-ICP-MS and are reported in Table 2. After this procedure, additional carbonate powders were collected for mineralogical determination by XRD at the Geology Department of the Free University of Brussels (Belgium) and confirmed that the shells consisted exclusively of aragonite.

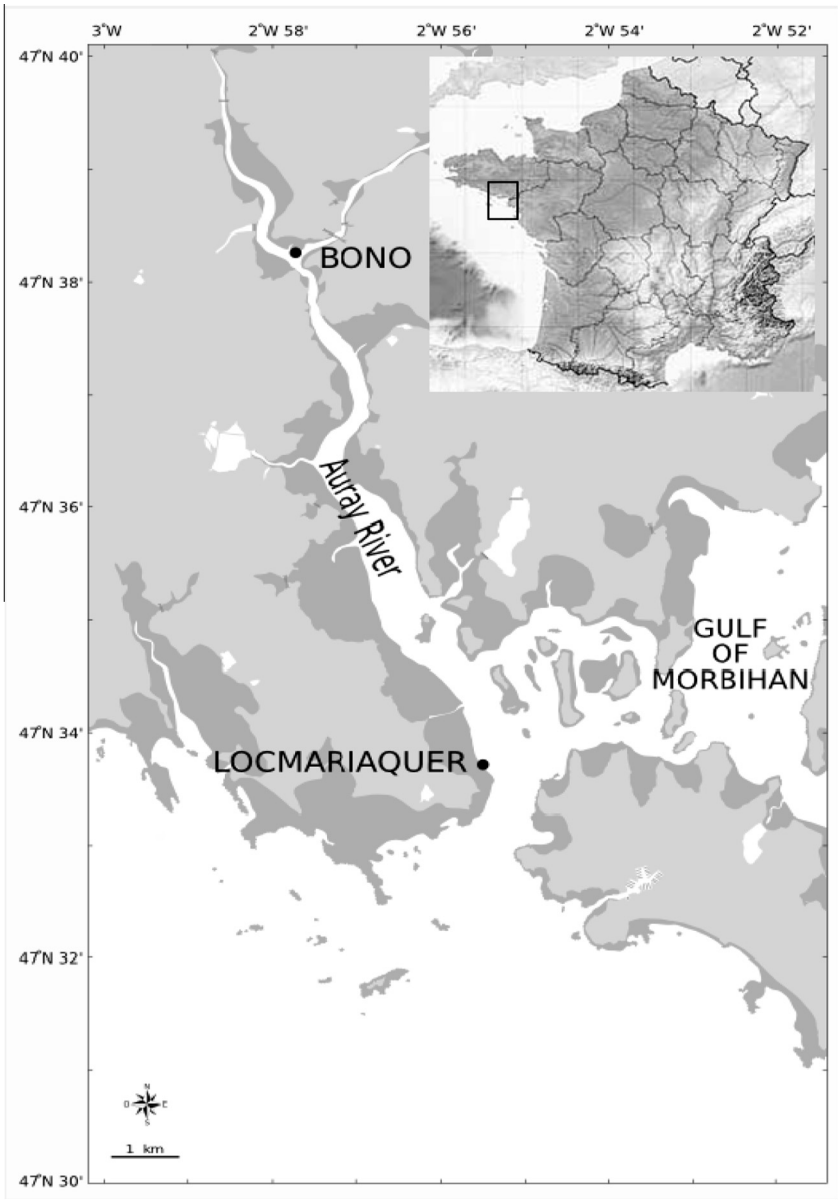

Fig. 1. Schematic map of two sampling sites along the Auray River (Le Bono and Locmariaquer) in the Gulf of Morbihan (France).

Growth period integrated by the carbonate samples taken from the outer prismatic layer was not determined in this study. Detailed analysis of growth dynamics was carried out at Le Bono from May to October 2007 using calcein markings on similar adult size clams (Poulain et al., 2011). Shell microgrowth increments are deposited with a tidal periodicity in the subtidal zone and mean lunar day growth rates vary between 20 and 50 μm lunar day^{-1} (Poulain et al., 2011). Consequently, the period integrated by the 1 mm growth increment may vary approximately between 20 and 50 days before collection.

2.2. Reference materials

In addition to field samples, a series of representative certified reference materials were chosen to reproduce the diversity of matrices considered in this study, and to control the quality of the measurements of Mg isotopic ratios and major ion concentrations. The series included a Coastal Atlantic Surface Seawater standard (CASS-4, National Research Council, Canada), a sample of oyster tissue (SRM 1566a, National Institute for Standards and Technology) and two marine biogenic aragonites: a coral *Porites* sp. (JCp-1, Geological Survey of Japan) and a giant clam *Tridacna gigas* (JCt-1, Geological Survey of Japan). The standards were processed in parallel to the samples, following the same procedures as described above and with comparable sample amounts: 100–200 μL for seawater CASS-4, ~50 mg of oyster tissue SRM 1566a and ~20 mg of calcium carbonates from JCp-1 (coral) and JCt-1 (giant clam). The concentrations of Mg, Ca, Na and K in the oyster tissue (SRM 1566a) and Mg/Ca and Sr/Ca ratios in the

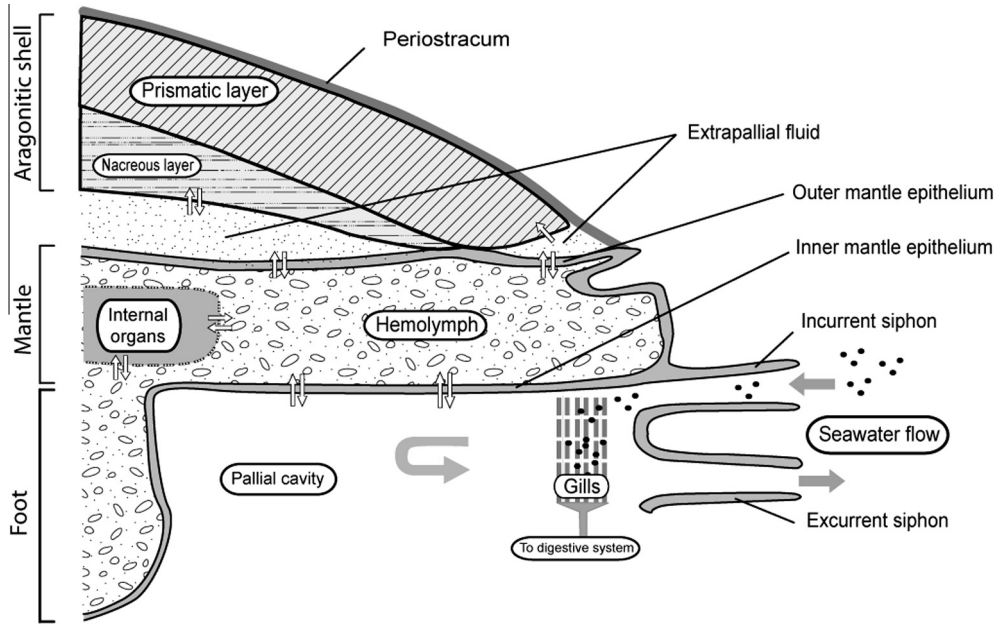

Fig. 2. Schematic lengthwise section through the ventral margin of a single valve of *R. philippinarum*, showing internal fluids (hemolymph and EPF), soft tissues (mantle, foot, gills and internal organs) and shell layers. Seawater flow (grey arrows) enters the pallial cavity by the incurrent siphon and is expelled by the excurrent siphon. White arrows illustrate potential transfer pathways of Mg from filtered seawater in the pallial cavity (pallial fluid) towards internal fluids, soft tissues and shell layers.

biogenic carbonates (JCp-1 and JCt-1) were determined by SF-ICP-MS and compared with certified values (Alvarez, 1990; Inoue et al., 2004). The average recoveries and associated precisions obtained were 97 ± 5% for Mg, Ca, Na and K in SRM 1566a, and 99 ± 7% for Mg/Ca and Sr/Ca ratios in carbonate standards. For the seawater standard CASS-4, not certified for major ions, the Mg, Ca, Na and K concentrations were deduced from the well-known seawater composition (Turekian, 1968) taking into account the lower salinity ($S = 30.7$ psu) in this coastal seawater. The measured concentrations in CASS-4 were on average 102 ± 5% of the calculated values for Mg (1132 μg g^{-1}), Ca (361 μg g^{-1}), Na (9473 μg g^{-1}) and K (344 μg g^{-1}).

2.3. Mg chemical purification

Reliable determination of Mg isotopic ratios using MC-ICP-MS requires the use of purified sample solutions to minimize instrumental mass bias created by Ar-plasma-interfering species (Galy et al., 2001; Wombacher et al., 2009). Modified from Chang et al. (2003), all chromatographic separations were performed with cationic-exchange resin (AG50W-X12, 200–400 mesh, H^+ form, Bio-Rad company) using a two-column procedure which allows full Mg purification from matrix-derived elements Na, K, Ca and Sr and guarantees a complete recovery (>99.9%).

The resin was first cleaned by successive agitation and settling, three times with 6 M HCl and Milli-Q water followed by three times with Milli-Q water alone. At each step, fine particles were removed with the liquid and the resin was finally stored in water. Polyethylene columns were packed with 2 mL of pre-cleaned resin and washed three times with 10 mL of 6 M double-distilled HCl, followed by 10 mL of 1 M Suprapur HF. Each column was calibrated using a synthetic standard solution containing Na, Mg, K, Ca and Sr and prepared from mono-elemental solutions. A two-step procedure was developed to ensure full Mg purification.

For the first elution, the resin was conditioned with 5 mL of 1.2 M double-distilled HCl and the sample was loaded in 0.5 mL of 1.2 M HCl. After a 1 mL wash with 1.2 M HCl, the Na fraction was eluted with 11 mL of 1.2 M HCl followed by the Mg + K fraction obtained by adding 16 mL of 1.2 M HCl. After this step, 1 mL was further eluted to systematically check the absence of Mg and to prevent any changes in retention volume due to the ageing of the resin. Once collected, the Mg + K fraction was dried down and re-dissolved in 2 M HCl for the second step. Before the second elution, columns were rigorously cleaned with 10 mL of 10 M HCl followed by 10 mL of 6 M HCl and 5 mL of Milli-Q water, and then conditioned with 5 mL of 2 M HCl. The samples were loaded in 0.5 mL 2 M HCl and washed with 2 mL of 2 M HCl before the collection of the Mg fraction with 9 mL of 2 M HCl. As for the first column, 1 additional mL was finally eluted for quality control. All fractions obtained were dried down and re-dissolved in 2% (v/v) HNO_3 for elemental and isotopic analysis.

The concentrations of Na, Mg, K, Ca and Sr were determined by SF-ICP-MS, and allowed the full Mg yield (>99.9%) to be systematically checked for each sample. Total blank contributions for the whole procedure were evaluated to 0.15 ng for Mg and <0.5 ng for Na, Ca and Sr. This blank represents less than 0.1% of the lowest Mg mass of samples (~1 μg).

Table 1
Mg isotope values determined for standard test solution (in-house 1) and various reference materials, and comparison with literature data.

Standard	Material	δ^{26}Mg (‰ DSM3)	$\pm U_c$[a] (‰ DSM3)	δ^{25}Mg (‰ DSM3)	$\pm U_c$[a] (‰ DSM3)	Δ^{25}Mg (‰ DSM3)	N_m[b]	N_s[c]	Reference
In-house 1	Mono-elemental Mg solution	−5.85	0.09	−3.05	0.05	0.00	45	0	This study
DSM3 (purified)	Mono-elemental Mg solution	−0.02	0.07	−0.02	0.05	−0.01	4	1	This study
CASS-4	Seawater	−0.80	0.06	−0.42	0.04	0.00	11	3	This study
IAPSO	Seawater	−0.79	0.10	−0.41	0.06	0.00	20	5	1
		−0.75	0.13	−0.39	0.07	0.00	8		2
		−0.83	0.05	−0.40	0.04	0.03	5		2
		−0.89	0.18	–	–		20		3
		−0.80	0.05	−0.42	0.02	0.00	10		4
		−0.74	0.07	−0.37	0.04	0.02	4		5
		−0.83	0.11	−0.42	0.09	0.01			6
NASS-5	Seawater	−0.84	0.16	−0.43	0.07	0.01	8	3	1
BCR-403	Seawater	−0.89	0.06	−0.47	0.11	−0.01	3		7
		−0.96	0.03	−0.46	0.03	0.04	8		7
		−0.89	0.14	−0.51	0.08	−0.05	1		7
		−0.82	0.14	−0.42	0.08	0.01	1		7
		−0.87	0.14	−0.47	0.08	−0.02	1		7
JCp-1	Aragonitic coral (*Porites* sp.)	−2.02	0.11	−1.05	0.06	0.00	15	4	This study
		−2.01	0.22	−1.05	0.12	0.00	37	9	1
		−1.96	0.04	−1.03	0.02	−0.01	6		4
JCt-1	Giant clam (*Tridacna gigas*)	−2.80	0.11	−1.45	0.08	0.01	3	1	This study
SRM1566a	Oyster tissue	−0.23	0.07	−0.14	0.05	−0.02	3	1	This study

1: From Wombacher et al. (2009); 2: Pearson et al. (2006); 3: Pogge von Strandmann et al. (2008a,b); 4: Hippler et al. (2009); 5: Ra and Kitagawa (2007); 6: Chang et al. (2004); 7: Bolou-Bi et al. (2009).

[a] Uncertainty at 95% confidence interval (2σ).

[b] N_m = number of measurements.

[c] N_s = number of chemical separations.

2.4. Mass spectrometry

Mg isotope analyses were performed using a Nu plasma MC-ICP-MS (Nu Instruments™, UK) and standard sample bracketing (SSB) for mass bias drift correction. The sample introduction system consisted of a self-aspirating micro-concentric PFA nebulizer with an uptake rate of ~100 μL min^{-1} and an Aridus II desolvating system (Cetac™, UK). The Aridus II was operated with a PFA spray chamber heated to 110 °C, a PTFE desolvating membrane to 160 °C, and without N_2 to limit polyatomic interferences (Galy et al., 2001; Tipper et al., 2008b; Wombacher et al., 2009). Plasma and Aridus II gas flows, torch position, RF power and lens settings were tuned daily for optimal ion-beam sensitivity and stability. The three Mg isotopes were simultaneously measured with low mass resolution settings ($R = m/\Delta m$ ~300) using 3 of 12 Faraday collectors with 10^{11} Ω resistors, with ^{25}Mg positioned on the axial cup and ^{26}Mg and ^{24}Mg on the extreme cups of the high- and low-mass side of the multiple collector, respectively. Running solutions typically contained 50–100 ng mL^{-1} of Mg in 1% (v/v) HNO_3, yielding a sensitivity of 8–10 V on mass 24. Data acquisition for 1 isotopic ratio consisted of 40 individual measurements for a 400 s total integration time (i.e. 4 blocks of ten 10 s signal integrations after a 5 s baseline measurement and peak centring at the beginning of each block). For SSB, the Mg concentration of the sample was adjusted to match the standard solution within ±10% and the sample average isotopic ratio was bracketed by two standards. For one bracket, the data were accepted when the mass bias observed between the two standards was below 0.25‰ for ^{26}Mg/^{24}Mg. With this rejection criterion, 15% of the data were excluded for a total of 188 accepted brackets. To prevent memory effects, the system was cleaned between standard and sample using Milli-Q water for 30 s, 5% (v/v) HNO_3 for 30 s and finally 1% (v/v) HNO_3 for 4 min. Acidified blank solution signal intensity was on average less than 10 mV for ^{24}Mg and never exceeded 0.2% of the sample signals for the three isotopes. The results are expressed in the conventional delta notation as δ^{26}Mg and δ^{25}Mg, the permil deviation of the measured ^{26}Mg/^{24}Mg and ^{25}Mg/^{24}Mg ratios of samples against the reference standard DSM3 (Galy et al., 2003):

$$\delta^{x}\mathrm{Mg} = \left(\frac{(^{x}\mathrm{Mg}/^{24}\mathrm{Mg})_{\mathrm{sample}}}{(^{x}\mathrm{Mg}/^{24}\mathrm{Mg})_{\mathrm{DSM3}}} - 1 \right) \times 1000 \quad (1)$$

(with $x = 26$ or 25)

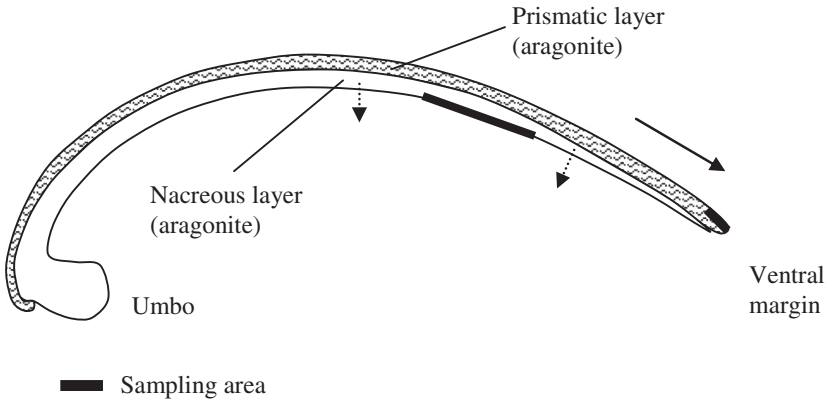

Fig. 3. Schematic cross section of the shell of *R. philippinarum* along the axis of maximal growth, showing the calcium carbonate sampling areas within the two aragonitic layers of the shell. Growth directions of the prismatic and nacreous layer are illustrated by solid and dotted arrows, respectively.

2.5. Precision and accuracy of δ^{26}Mg and δ^{25}Mg

Measurement precision was estimated by considering a combined uncertainty U_c composed of two contributions: the counting uncertainty U_{cnt} and the repeatability U_{rep} deduced from replicate analysis.

The instrumental uncertainties U_{cnt}, expressed as relative standard deviation in permil at 95% confidence interval, were available for each pair of δ^{26}Mg and δ^{25}Mg values and estimated by propagating the instrumental errors associated with each isotopic ratio through the delta equation:

$$U_{cnt}(\delta^x\mathrm{Mg}) = k \times 1000 \times \sqrt{\left(\frac{\sigma R_{x,\mathrm{std1}}}{R_{x,\mathrm{std1}}}\right)^2 + \left(\frac{\sigma R_{x,\mathrm{std2}}}{R_{x,\mathrm{std2}}}\right)^2 + \left(\frac{\sigma R_{x,\mathrm{sple}}}{R_{x,\mathrm{sple}}}\right)^2} \quad (2)$$

with $x = 26$ referring to ^{26}Mg/^{24}Mg ratio and $x = 25$ to ^{25}Mg/^{24}Mg ratio; k is the coverage factor (= 2) used for the 95% confidence interval estimate. $\sigma(R_{x,\mathrm{sple}})$, $\sigma(R_{x,\mathrm{std1}})$ and $\sigma(R_{x,\mathrm{std2}})$ represent the instrumental standard errors obtained for the sample isotopic ratio ($R_{x,\mathrm{sple}}$) and the two bracketing standards, $R_{x,\mathrm{std1}}$ and $R_{x,\mathrm{std2}}$, respectively. In this study, the instrumental uncertainty U_{cnt} ranged for δ^{26}Mg from 0.02‰ to 0.08‰ (average = 0.04‰, $n = 188$ brackets) and for δ^{25}Mg from 0.02‰ to 0.06‰ (average = 0.03‰, $n = 188$ brackets).

The repeatability component U_{rep} represents twice the standard deviation associated with the average delta value obtained for n replicates. Replicates included repeated measurements of all samples processed through chemical purification. Numbers of measurement and chemical separation are reported in Table 1 for reference materials and in Tables 2 and 3 for samples. Considering all standards and samples, U_{rep} showed a range of 0.04–0.13‰ (average = 0.09‰, $n = 38$ results) for δ^{26}Mg and of 0.02–0.09‰ (average = 0.04‰, $n = 38$ results) for δ^{25}Mg.

Finally, the combined uncertainty U_c in permil at 95% confidence interval accounted for the two contributions using the Root-Sum-Square (RSS) method:

$$U_c(\delta^x\mathrm{Mg}) = \sqrt{\bar{U}_{cnt}(\delta^x\mathrm{Mg})^2 + U_{rep}(\delta^x\mathrm{Mg})^2} \quad (3)$$

where x refers either to 26 or 25, and $\bar{U}_{cnt}(\delta^x\mathrm{Mg})^2$ is the average counting uncertainty for n (δ^xMg) replicates. U_c values are reported in Tables 1–3.

The long-term (i.e. over 2 years) internal precision was evaluated with a non-purified, in-house, mono-elemental Mg standard (Alfa Aesar, Johnson Matthey Company) and U_c was 0.09‰ and 0.05‰ ($n = 45$) for δ^{26}Mg and δ^{25}Mg. For the reference materials processed through chemical purification comparable precisions were found (Table 1), with U_c of 0.07‰ and 0.05‰ for purified DSM3 ($n = 4$), 0.06‰ and 0.04‰ for seawater CASS-4 ($n = 11$), 0.11‰ and 0.06‰ for aragonitic coral JCp-1 ($n = 15$), 0.11‰ and 0.08‰ for aragonitic clam JCt-1 ($n = 3$), and 0.07‰ and 0.05‰ ($n = 3$) for oyster tissue SRM 1566a in δ^{26}Mg and δ^{25}Mg, respectively. For samples, U_c were also similar and ranged from 0.04‰ to 0.13‰ for δ^{26}Mg and from 0.02‰ to 0.09‰ for δ^{25}Mg.

In terms of accuracy and as illustrated in Table 1, the delta values determined in this study for seawater (CASS-4) and coral standards (JCp-1) closely agree with published data obtained for other natural seawater reference materials (Chang et al., 2004; Pearson et al., 2006; Ra and Kitagawa, 2007; Pogge von Strandmann et al., 2008b; Bolou-Bi et al., 2009; Hippler et al., 2009; Wombacher et al., 2009) and also for carbonate standard JCp-1 (Hippler et al., 2009; Wombacher et al., 2009).

3. RESULTS

Results obtained for seawater, the *R. philippinarum* samples, and reference materials are listed in Tables 1–3 and presented in Fig. 4. Overall variation of the samples is 4.16‰ and 2.16‰ in δ^{26}Mg and δ^{25}Mg, respectively. This is about 30 times the highest measurement uncertainty

Table 2
Mg isotopic ratios and Mg, Ca, Na, and K concentrations in seawater, internal fluids and soft tissues of manila clam *R. philippinarum* at the two sampling sites.

Location	Sample	Description	Specimen #	δ^{26}Mg (‰ DSM3)	$\pm U_c$[a] (‰ DSM3)	δ^{25}Mg (‰ DSM3)	$\pm U_c$[a] (‰ DSM3)	Δ^{25}Mg′ (‰ DSM3)	N_m[b]	N_s[c]	Concentrations in ppm[d]			
											Mg	Ca	Na	K
Locmariaquer	Seawater			−0.82	0.09	−0.42	0.06	0.01	3	1	1269	411	10,726	383
				−0.85	0.09	−0.45	0.05	0.00	3	1	1198	391	10,238	385
	Internal fluids	EPF	L1	−0.98	0.11	−0.50	0.05	0.01	3	2	1165	499	10,090	381
		Hemolympli	L1	−0.95	0.14	−0.48	0.07	0.01	5	2	1154	476	9960	388
	Soft tissues	Mantle	L1	−0.40	0.08	−0.22	0.05	−0.01	4	1	4082	2132	24,234	11,417
		Muscle	L1	−0.36	0.08	−0.19	0.04	0.00	3	1	2358	1655	12,143	7234
		Other	L1	−0.12	0.12	−0.06	0.05	0.01	3	1	3259	2338	17,461	13,396
Le Bono	Seawater			−0.79	0.10	−0.41	0.05	0.00	3	1	1115	368	9544	370
				−0.81	0.07	−0.42	0.02	0.01	3	1	1079	348	9335	340
	Internal fluids	EPF	B1	−0.89	0.09	−0.46	0.04	0.00	3	1	971	383	8606	352
		EPF	B2	−1.15	0.10	−0.61	0.06	−0.01	6	2	978	394	8508	350
		EPF	B3	−1.19	0.14	−0.62	0.08	0.00	3	1	942	386	8346	344
		EPF	B4	−1.02	0.08	−0.53	0.04	0.00	3	1	953	404	8406	331
		Hemolymph	B1	−0.89	0.14	−0.47	0.07	−0.01	3	1	940	368	8352	336
		Hemolymph	B2	−0.99	0.09	−0.52	0.06	0.00	3	1	981	396	8512	333
		Hemolymph	B3	−1.23	0.09	−0.63	0.06	0.01	3	1	919	364	8176	349
		Hemolymph	B4	−0.98	0.12	−0.50	0.07	0.01	3	1	987	399	8694	343
	Soft tissues	Mantle	B2	−0.31	0.12	−0.16	0.06	0.00	3	1	3052	1748	13,233	12,229
		Muscle	B2	−0.30	0.07	−0.17	0.05	−0.01	3	1	1696	986	7206	9179
		Other	B2	−0.06	0.08	−0.04	0.03	0.00	3	1	2163	1080	8756	14,559

[a] Uncertainty are at 95% confidence interval (2σ).
[b] N_m = number of measurements.
[c] N_s = number of chemical separations.
[d] Concentrations are expressed per unit mass of liquid for seawater and internal fluids, and per unit mass of dry weight for soft tissues; values are at 5% RSD.

and it represents approximatively two-thirds of the terrestrial range so far identified (Galy et al., 2002; Chang et al., 2004; Young and Galy, 2004; Black et al., 2006, 2008; Pearson et al., 2006; Tipper et al., 2006; Buhl et al., 2007; Ra and Kitagawa, 2007; Pogge von Strandmann, 2008; Pogge von Strandmann et al., 2008a,b; Tipper et al., 2008a,b; Bolou-Bi et al., 2009; Hippler et al., 2009; Wombacher et al., 2011). Within the uncertainties, linearized delta values δ^{26}Mg′ and δ^{25}Mg′ (Young and Galy, 2004) of the samples define a single mass-dependent fractionation line ($r = 0.999$, $n = 32$, $p < 0.0001$). The slope of the linear trend ($\beta = 0.519 \pm 0.002$) is identical within error to the theoretical equilibrium exponential fractionation factor of 0.521 (Young et al., 2002). Deviation from this law for each delta value is expressed as Δ^{25}Mg′ (Young et al., 2002) and is reported in Tables 1–3. All results are consistent with the equilibrium isotope fractionation within analytical uncertainty and we will hereafter only refer to δ^{26}Mg.

3.1. Seawater

The seawater samples from the Gulf of Morbihan have a mean δ^{26}Mg of -0.82 ± 0.09‰ ($n = 4$). The two sampling sites with different salinities at high tide (30.2 psu at Bo and 33.7 psu at Loc) have indistinguishable mean δ^{26}Mg = -0.80 ± 0.09‰ ($n = 2$) at Le Bono and δ^{26}Mg = -0.84 ± 0.09‰ ($n = 2$) at Locmariaquer. Results closely agree with the seawater reference material CASS-4 (-0.80 ± 0.06‰), determined in this study, and literature data for other seawater reference materials as listed in Table 3. It is also similar to open-ocean signatures of Mg isotopes measured for a number of ocean basins: -0.82 ± 0.06‰ (Foster et al., 2010), observed in the Atlantic and the Mediterranean: -0.83 ± 0.14‰ (Chang et al., 2004; Young and Galy, 2004); the North Pacific: -0.83 ± 0.22‰ (Ra and Kitagawa, 2007); coastal areas in the North Sea: -0.79 ± 0.03‰ (Hippler et al., 2009); Iceland: -0.82 ± 0.18‰; and the Azores: -0.84 ± 0.18‰ (Pogge von Strandmann et al., 2008b).

Since the two sampling sites are in different salinity regimes, Mg isotopic composition of seawater could vary according to the tide and freshwater inputs from the Auray River. Neither the Auray River nor seawater at low tide were sampled in this study, so such variations cannot be precisely assessed. However, Mg and its isotopes behave as non-reactive species in estuarine environments (Pogge von Strandmann et al., 2008b) so that any potential variations in water δ^{26}Mg can be predicted from salinity fluctuations. We consider a simple binary mixing model with (as end-members) seawater (δ^{26}Mg = -0.82 ± 0.09‰ and [Mg] = 53 mmol L^{-1}) and the Auray River, defined conservatively by the highest dissolved Mg content reported for world rivers [Mg] = 0.9 mmol/l (Tipper et al., 2006) and an array of δ^{26}Mg between 0‰ and −1.5‰ corresponding to rivers draining silicate rocks (Brenot et al., 2008; Tipper

Table 3
Mg isotopic, Mg/Ca and Sr/Ca ratios in selected parts of the aragonitic shell of the manila clam *R. philippinarum* at the two sampling sites.

Location	Individual	Shell layer	Valve	Growth increment[a] (mm)	δ^{26}Mg (‰ DSM3)	$\pm U_c$ (‰ DSM3)[b]	δ^{25}Mg (‰ DSM3)	$\pm U_c$ (‰ DSM3)[b]	Δ^{25}Mg′ (‰ DSM3)	N_m[c]	N_s[d]	Mg/Ca (mmol/mol)[e]	Sr/Ca (mmol/mol)[e]
Locmariaquer	L1	Prismatic	Left	0–1	−1.89	0.07	−1.00	0.05	−0.01	4	2	1.1	1.7
		Prismatic	Left	1–2	−1.97	0.08	−1.04	0.05	−0.01	5	2	1.3	1.7
		Nacreous	Left	–	−2.14	0.13	−1.10	0.07	0.01	3	1	1.3	1.7
		Prismatic	Right	0–1	−2.16	0.10	−1.13	0.06	0.00	3	1	1.3	1.7
		Nacreous	Right	–	−2.75	0.08	−1.43	0.04	0.00	3	1	0.9	1.5
Le Bono	B1	Prismatic	Left	0–1	−2.47	0.07	−1.28	0.04	0.01	3	1	1.2	1.6
		Nacreous	Left		−3.18	0.10	−1.63	0.06	0.02	3	1	0.6	1.4
	B2	Prismatic	Left	0–1	−3.98	0.12	−2.09	0.07	−0.01	3	1	0.8	1.5
		Prismatic	Left	1–2	−2.17	0.13	−1.14	0.09	−0.01	3	1	1.2	1.6
	B3	Prismatic	Left	0–1	−2.43	0.08	−1.24	0.07	0.02	3	1	1.1	1.6
		Nacreous	Left		−3.02	0.12	−1.56	0.06	0.02	3	1	0.4	1.9
	B4	Prismatic	Left	0–1	−4.22	0.06	−2.20	0.04	0.00	5	2	0.9	1.4

[a] From the ventral margin and along the maximum growth axis.
[b] Uncertainty at 95% confidence interval (2σ).
[c] N_m = number of measurements.
[d] N_s = number of chemical separations.
[e] Molar ratios are at 7% RSD.

et al., 2008a). We estimate that significant changes in δ^{26}Mg of the surrounding seawater could occur only at the brackish water site Le Bono, with δ^{26}Mg potentially varying between −0.70‰ and −0.92‰ at the annual salinity minimum (i.e. 3 psu) and potentially differing by ±0.12‰ from seawater δ^{26}Mg.

3.2. Internal fluids

The Mg-isotopic composition obtained from hemolymph and EPF samples are listed in Table 2 and presented in Fig. 5. The hemolymph, which represents the intercellular fluid of soft tissue, have δ^{26}Mg of -0.95 ± 0.14‰ in the individual L1 collected at Locmariaquer and varying from -0.89 ± 0.14‰ to -1.23 ± 0.09‰ in the four individuals (B1 to B4) collected at Le Bono. For L1, B1, B2, and B4, δ^{26}Mg of hemolymph cannot be distinguished from the seawater end-member with our analytical precision. By contrast, hemolymph δ^{26}Mg in individual B3 appears to be 0.41‰ lighter than seawater and indicates light isotope enrichment. The EPF is considered to be the microenvironment for deposition of the bivalve shell (Wheeler, 1992); it occupies the extrapalleal space between the inner shell surface and the outer mantle epithelium (Crenshaw, 1972). As shown in Fig. 5, EPF samples exhibit a Mg-isotopic composition very similar to hemolymph, with δ^{26}Mg of -0.98 ± 0.11‰ (L1) at Locmariaquer and between -0.89 ± 0.09‰ (B1) and -1.19 ± 0.14‰ (B3) at Le Bono (Fig. 4). Isotopic identity with seawater is observed in L1 and B2 but not in B2, B3, and B4, which show light isotope enrichment of −0.33‰, −0.37‰, and −0.20‰, respectively.

Mg, Ca, Na and K concentrations in EPF and hemolymph (Table 2) are all very similar and are homogeneous with our analytical precision (5%) for the four individuals from Le Bono. The concentrations show a systematic decrease between the two sites; the lower values observed at Le Bono (~16% on average) reflect the 10% lower salinity of seawater at this site. The body fluids exhibit only minor differences in major cation abundances relative to seawater at each site. At Locmariaquer: 5% lower for Mg and Na, equal for K, and 22% higher for Ca; at Le Bono: 12% lower for Mg and Na, 4% for K and 8% higher for Ca. As illustrated in Fig. 5, element-to-Na ratios in hemolymph and EPF are consistent with an oceanic fingerprint for Mg/Na and K/Na but not for Ca/Na, which is significantly higher. These results agree with previous estimates of element-to-Na ratios in EPF (Crenshaw, 1972) and in mantle fluids (Shakhmatova et al., 2006) from various species of marine bivalves.

3.3. Organic tissues

The Mg isotopic composition of soft tissues, which include the mantle, muscle and remaining organs, were determined for two specimens (L1 and B2) and have the heaviest Mg isotopic composition of the dataset. The δ^{26}Mg values vary between -0.06 ± 0.08‰ and -0.40 ± 0.08‰ (Table 2) so that all soft tissues are enriched, to varying degrees, in the heavy isotope relative to seawater. Average Mg isotopic composition of the mantle (-0.36 ± 0.08‰, $n = 2$) and muscle (-0.33 ± 0.10‰, $n = 2$) are comparable, and differ by 0.48 ± 0.09‰ from seawater δ^{26}Mg. The remaining organs (average: -0.09 ± 0.08‰, $n = 2$) are significantly heavier and differ from seawater by 0.72 ± 0.09‰. Considering the two specimens L1 and B2, no differences in δ^{26}Mg are observed for the mantle, muscle or other organs (Table 1). The average δ^{26}Mg for the soft tissues is -0.26 ± 0.09‰ (3 fractions from 2 individuals, $n = 6$).

Major cation concentrations in organic tissues (expressed per dry weight) are notably higher than in internal fluids and seawater (Table 2). This is especially the case for K, which shows a 29-fold increase on average in the organic

fraction, but it concerns also Mg and Ca, which have increase factors of 2.1 and 4.0, respectively. The cationic budget of tissues appears variable between organs and individuals; it is dominated by Na and K alternatively, followed by Mg and finally Ca. Average element-to-Na ratios (Mg/Na = 0.21 g/g; Ca/Na = 0.13 g/g; K/Na = 0.95) do not compare with seawater or internal fluids (Mg/Na = 0.12 g/g; Ca/Na = 0.04 g/g; K/Na = 0.04) but compare with certified values for oyster tissue (Mg/Na = 0.28 g/g; Ca/Na = 0.47 g/g; K/Na = 1.9 g/g) and also with average data for soft tissues obtained from other bivalves, such as *M. edulis* and *Mytilus trossulus* (Mg/Na = 0.21 g/g; Ca/Na = 0.14 g/g; K/Na = 1.7 g/g) (Shakhmatova et al., 2006).

3.4. Aragonitic shells

The samples of clam shell show the lightest Mg-isotopic composition and also the largest variability, ranging from $-1.89 \pm 0.07‰$ to $-4.22 \pm 0.06‰$ (Table 3). As shown in Fig. 6, inter- and intra-individual variability of shell δ^{26}Mg is particularly large. In L1, the left valve exhibits similar δ^{26}Mg, with $-1.89 \pm 0.07‰$ in the 0–1 mm growth increment, $-1.97 \pm 0.08‰$ in the 1–2 mm growth increment and $-2.14 \pm 0.13‰$ in the nacreous layer. In the right valve, δ^{26}Mg appears lighter in both the prismatic ($-2.16 \pm 0.10‰$) and the nacreous ($-2.75 \pm 0.08‰$) layers. Shell samples obtained from Le Bono exhibit systematically lighter Mg-isotopic composition compared to Locmariaquer, except in the 1–2 mm growth increment of B2. In B1 and B3 the 0–1 mm growth increment, which represents the most-recently precipitated part of the prismatic shell yield similar δ^{26}Mg of $-2.47 \pm 0.07‰$ (B1) and $-2.43 \pm 0.08‰$ (B3). By contrast, δ^{26}Mg obtained from the same growth increment appears substantially lighter in B2 ($-3.98 \pm 0.12‰$) and B4 ($-4.22 \pm 0.06‰$). At Le Bono, nacreous samples have δ^{26}Mg of $-3.18 \pm 0.10‰$ (B1) and $-3.02 \pm 0.12‰$ (B3), and appear 0.71‰ and 0.59‰ lighter than the prismatic layer obtained from the same individual.

As shown in Fig. 6, the array of Mg isotopic compositions obtained from aragonitic shells of *R. philippinarum* ($-1.89 \pm 0.07‰$ to $-4.22 \pm 0.06‰$, $n = 12$) encompasses the domains defined by various modern marine calcifiers. It includes the two biogenic carbonate reference materials determined in this study: the aragonitic coral JCp-1 at $-2.02 \pm 0.11‰$ and aragonitic giant clam JCt-1 at $-2.80 \pm 0.11‰$, as well as the signatures observed in brachiopods, echinoids, red algae, deep-sea coral and the bivalve *M. edulis* (Chang et al., 2004; Hippler et al., 2009). Our data indicate that manila clam shells remain heavier than strongly fractionated mixed species of foraminifers (Chang et al., 2004; Pogge von Strandmann, 2008).

4. DISCUSSION

Mg isotopic compositions obtained from the different constituents of the euryhaline bivalve *R. philippinarum* exhibit an overall δ^{26}Mg variability of 4.16‰. This contrasts with the relatively stable Mg isotopic composition of the brackish waters studied, for which only limited fluctuations (±0.12‰) relative to the open-ocean signature may be expected. As Mg assimilated by marine invertebrates is commonly assumed to come from surrounding seawater (Klein et al., 1996b) due to its high abundance and free-divalent form readily available for cells (Maguire and Cowan, 2002), the present dataset clearly demonstrates that mass-dependent fractionation occurs during the transfer of Mg within the organism. In order to identify controlling factors of this partitioning that vary according to the compartment involved, current knowledge of Mg incorporation pathways in bivalves needs to be briefly outlined.

4.1. Bivalve anatomy and Mg incorporation

A schematic picture of the clam and principal Mg transfer routes from the surrounding environment to the internal compartments and shell layers are illustrated in Fig. 2. Mg is introduced into the bivalve organism via the seawater current created in the pallial cavity for filter feeding. Seawater is pumped through the incurrent siphon, travels across the gills collecting suspended material and dissolved oxygen, and is finally expelled through the excurrent siphon. The pallial fluid, filling the pallial cavity, is continuously renewed with filtered seawater and represents the primary Mg source for biological uptake and shell formation.

The first incorporation step is controlled by the mantle and takes place at the inner mantle epithelium (IME), a thin membrane composed of epithelial cells joined by connective tissues that surrounds the body of the animal and is in contact with the pallial fluid. The IME allows trans-epithelial transport of Mg towards the hemolymph side, which represents the intercellular compartment. The hemolymph acts as bathing fluid for internal organs and cells, and as a blood analogue in the bivalve open-circulatory system (Eble and Scro, 1996). The hemolymph circulation promotes dissolved Mg distribution within the soft tissue, and hence further exchange with other compartments. By crossing the membrane of mantle and muscle cells and/or specific epithelia of internal organs, Mg can reach the intracellular medium, where it plays a key role as a nutrient and determines numerous enzymatic and cellular processes (e.g. Maguire and Cowan, 2002; Romani and Maguire, 2002; Wolf et al., 2003).

From the hemolymph compartment, Mg can also be transferred to the shell-forming extrapallial fluids (EPF) located in the extrapallial cavities, where biomineralization takes place. The secretion of EPF and transfer of shell-forming elements (Ca^{2+}, Mg^{2+}, CO_3^{2-}) are controlled by the outer mantle epithelium (OME) (Crenshaw, 1980), which plays a central role in the formation of the shell. Specialized epithelial cells secrete a macromolecular matrix which actively induces biomineralization (Mount et al., 2004; Addadi et al., 2006; Jacob et al., 2008). During this biologically mediated process, Mg in EPF can be incorporated and stored as a minor component in the precipitated skeletal hard parts.

Mg isotopic data obtained along this complex incorporation pathway will be used in the following sections to pro-

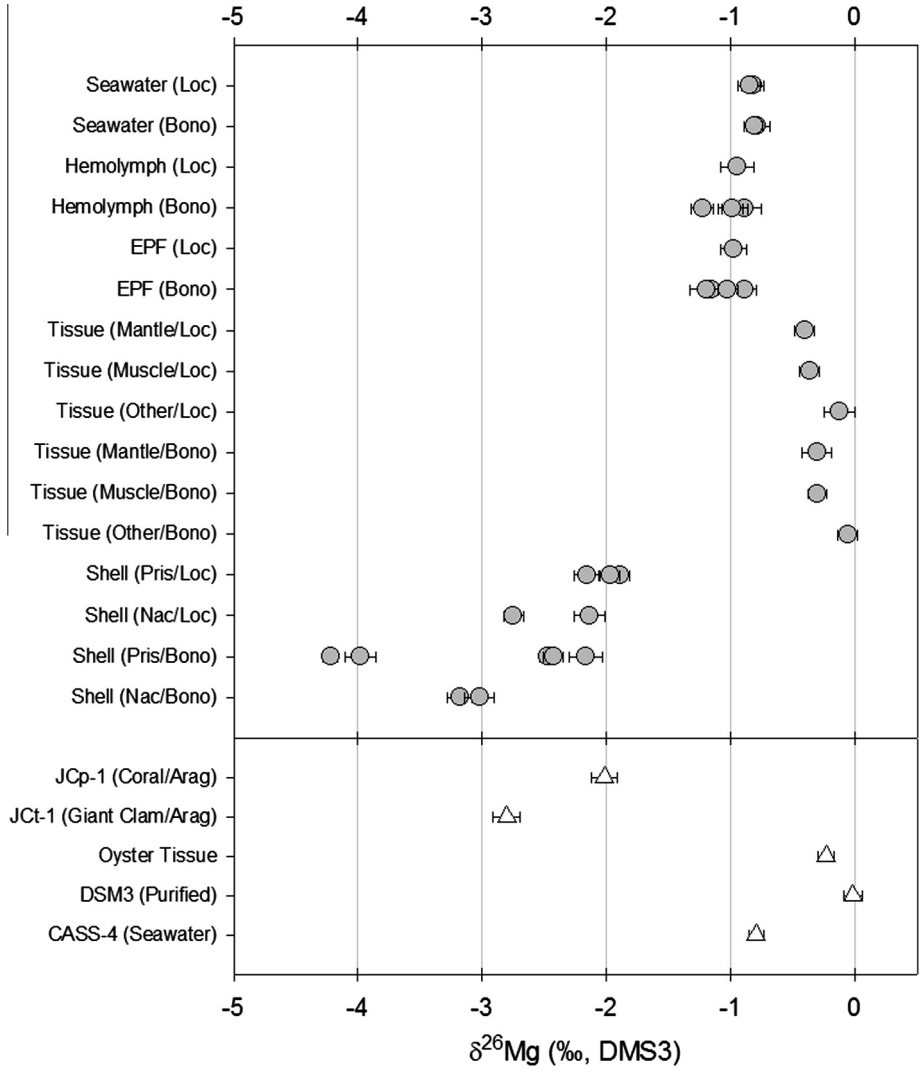

Fig. 4. Measured δ^{26}Mg (‰ vs. DSM3) for seawater, extrapallial fluid (EPF), hemolymph, soft tissues, prismatic and nacreous aragonitic shells of the manila clam (*R. philippinarum*) collected at the two sampling sites (Locmariaquer and Le Bono). Also shown, measured δ^{26}Mg (‰ vs. DSM3) of reference materials JCp-1 (aragonitic coral), JCt-1 (aragonitic giant clam), oyster tissue (SRM 1566a), DSM3 purified through column chemistry, and CASS-4 (coastal seawater).

vide relevant constraints on biological controls occurring in the bivalve biomineralisation process.

4.2. Fractionation in bivalve soft tissues

Mg exchanges across the biological compartments of the clam account for a significant fraction of δ^{26}Mg variability. The fractionation factor between the hemolymph and the soft tissues ($\Delta^{26}Mg_{soft\ tissue\text{-}hemolymph}$) varies from 0.53 ± 0.16‰ (specimen L1) to 0.93 ± 0.12‰ (specimen B2) and points to a biological fractionation of Mg isotopes. If we assume that solid organic samples are representative of the intracellular medium, the Mg isotopic fractionation may be related to the incorporation process within the cell. This assumption is supported by the potassium enrichment observed in the soft tissues (mean $K/Na = 0.61 \pm 0.15$, $n = 3$ at Loc and 1.29 ± 0.37, $n = 3$ at Le Bono) compared to the hemolymph ($K/Na = 0.038 \pm 0.003$ at Loc and mean $K/Na = 0.041 \pm 0.003$, $n = 4$ at Le Bono). K enrichment reflects the selective transport of K over Na performed at the cell membrane by Na/K exchangers, and is documented for most living organisms including marine bivalves (Shakhmatova et al., 2006). However, it is worth mentioning that despite the successive rinsing steps applied to the solid organic samples during sample preparation, a limited contribution of intercellular Mg cannot be excluded. Considering the lighter isotopic ratios found in hemolymph (-0.95‰ at Loc and -1.02‰ at Le Bono) relative to the soft tissues samples (-0.30‰ at Loc and -0.22‰ at Le Bono), the δ^{26}Mg value of the soft tissues has to be considered as a lower limit for the Mg isotopic composition of the intracellular medium.

When compared to the seawater δ^{26}Mg that can be defined as the parent fluid signature, soft tissues and

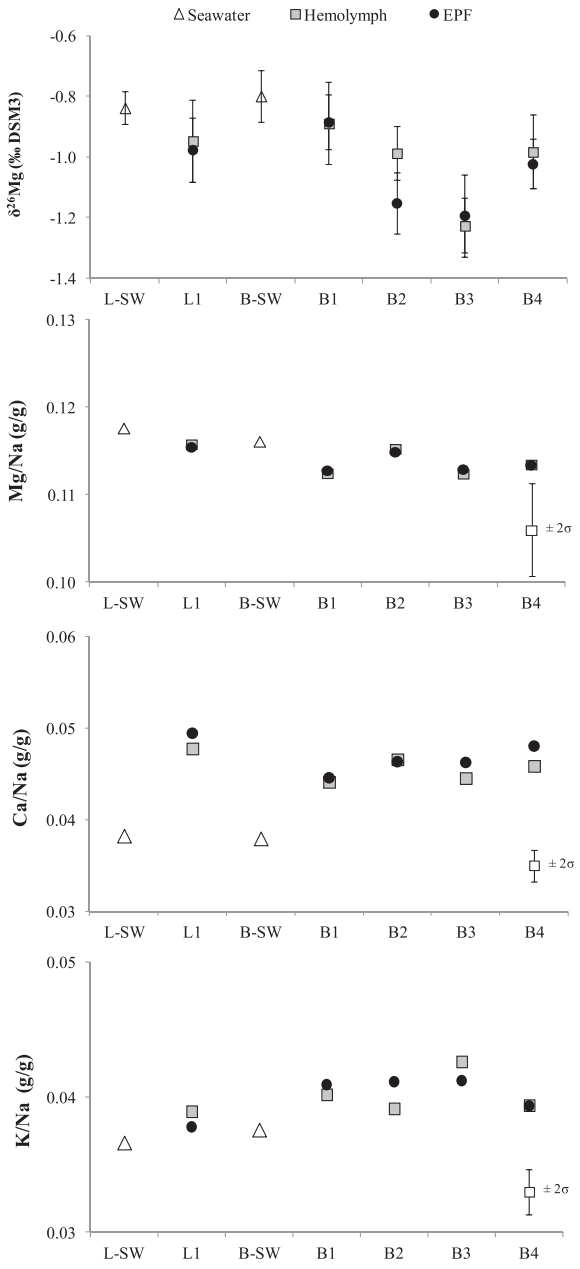

Fig. 5. δ^{26}Mg (‰ vs. DSM3), and Mg/Na, Mg/Ca, and K/Na mass ratios in the extrapallial fluid (EPF) and hemolymph of individuals collected at Locmariaquer (L1) and Le Bono (B1 to B4) and comparison with seawater data obtained at each site (L-SW and B-SW). Errors bars refer to 95% confidence interval.

hemolymph display distinct fractionation patterns (Fig. 8). The hemolymph samples, with $\Delta^{26}Mg_{hemolymph\text{-}seawater}$ of -0.13 ± 0.14‰ at Loc and -0.20 ± 0.28‰ (2 sd, $n = 4$) at Le Bono, stay close to the seawater end-member over the analytical uncertainty. By contrast, the soft tissue samples, with $\Delta^{26}Mg_{soft\ tissue\text{-}seawater}$ of 0.42 ± 0.12‰ to 0.76 ± 0.12‰, are fractionated towards heavy isotope compositions relative to seawater. Fractionation is of similar magnitude in the mantle ($\Delta^{26}Mg_{soft\ tissues\text{-}seawater} = 0.46 \pm 0.17$‰, 2 sd, $n = 2$) and in the adductor muscle (0.49 ± 0.19‰, 2 sd, $n = 2$), and is higher in the visceral mass (0.73 ± 0.20‰, 2 sd, $n = 2$). Between the two sampling sites, $\Delta^{26}Mg_{soft\ tissues\text{-}seawater}$ remains unchanged for each organ although Mg concentration is 25 to 34% lower in the solid organic samples from Le Bono (see Table 2). Such a decrease in Mg concentration may be due to the lower salinity conditions at Le Bono (Shakhmatova et al., 2006). Mg isotopic fractionation identified in the soft parts of the manila clam compares well with bulk oyster tissue (SRM1566a: see Table 1) and may represent a common feature of marine bivalves.

The observed heavy Mg isotopic enrichment in organic tissues indicates that the processes regulating Mg transfer and sequestration into the cell may act as a key fractionation step. Mg transport through the cellular membrane requires, as for other cations, specific ion-transporter mechanisms (Flatman, 1984); passive diffusion through the lipid bilayer membrane is hindered by the large size of the hydrated ion (Maguire and Cowan, 2002). This active transport of Mg can take several forms and can be mediated either by Mg-specific channels (Warren et al., 2004; Maguire, 2006) or by other ionic regulation systems such as Na/K exchangers, Ca channels or other voltage-gated channels (Flatman, 1984; Yago et al., 2000; Nadler et al., 2001; Konrad et al., 2004; Hoenderop and Bindels, 2008). Each of these mechanisms implies Mg binding to various organic substrates, and may be of importance in the observed isotopic fractionation. Isotopic selection associated with Mg chelate formation is well documented for sulfonated (Chang et al., 2003; Teng et al., 2007) and peptide resins (Kim and Kang, 2001; Kim et al., 2003) and is consistent with Mg isotope fractionation associated with chlorophyll synthesis (Black et al., 2006). However, such complexation processes favour the light isotope of Mg and therefore cannot explain the opposite trends observed in the bivalve soft tissues. In this light, the recently discovered Mg "Transient Receptor Potential" channels (Warren et al., 2004; Van der Wijst et al., 2009) offer alternative characteristics. In contrast to resin functional groups and the Mg-chelatase enzyme (Walker and Willows, 1997), the large size of the transport protein's Mg binding site allows the insertion of the fully hydrated Mg ion. In this case, Mg isotope fractionation could arise from the different Mg–O bond-strengths of the Mg-aquocomplex. The more stable hydration sphere formed with the heavier isotopes (higher dissociation energy) could be preferred for chelation in combination with the transport protein and hence, for transfer inside the cell. This hypothesis for marine bivalves may be valid also for plant cells (Black et al., 2008; Bolou-Bi et al., 2010) and for some marine phytoplankton species (Ra and Kitagawa, 2007) where similar heavy isotope enrichments are observed.

4.3. Mg isotopes in the hemolymph

In the hemolymph, a mean fractionation factor $\Delta^{26}Mg_{hemolymph\text{-}seawater}$ of -0.20 ± 0.27‰ (2 sd, $n = 5$) indicates no difference with parent seawater within our analytical precision. This supports a predominant seawater origin for Mg in hemolymph, and highlights the role of the active osmoregulation process, which maintains

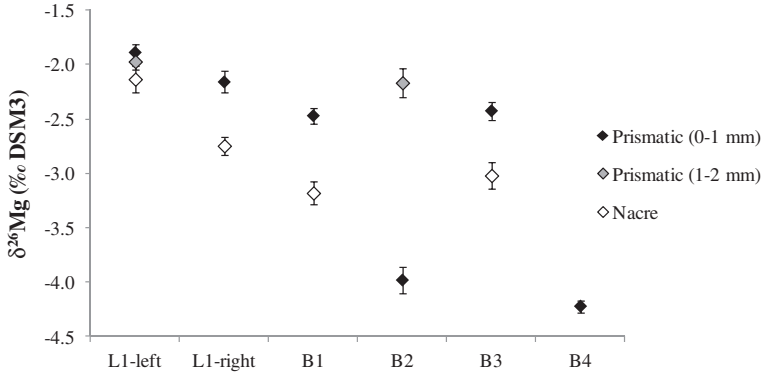

Fig. 6. $\delta^{26}Mg$ (‰ vs. DSM3) in prismatic and nacreous shell components of individuals collected at Locmariaquer (L1) and Le Bono (B1 to B4). L1-left and L1-right refers to the left and right valve, respectively of individual L1. Prismatic 0–1 mm and prismatic 1–2 mm refers to the 0–1 and 1–2 mm growth increment sampled from the ventral margin and along the maximal growth axis.

near-chemical equilibrium with the surrounding environment in osmoconformers such as bivalves (Crenshaw, 1972; Neufeld and Wright, 1996, 1998; Berger and Kharazova, 1997; Shakhmatova et al., 2006). The lack of substantial fractionation in hemolymph indicates that the trans-epithelial transport of Mg through the IME (from pallial fluid to hemolymph) is relatively passive. This may be consistent with a preferential transfer route via paracellular pathways at septate junctions (Lord and DiBona, 1976; Klein et al., 1996b).

However, for one hemolymph sample (B3) $\Delta^{26}Mg_{hemolymph\text{-}seawater}$ is -0.41 ± 0.09‰, suggesting that limited isotopic controls cannot be rigorously excluded. Such controls may involve a trans-cellular component in Mg trans-epithelial transport as well as other internal processes such as adsorption/desorption equilibrium on cell surface or organic molecules, and Mg incorporation into the soft tissues. As discussed in the previous section, the latter process preferentially incorporates heavy isotope in the soft tissues, leaving light isotopes in the hemolymph and this fits with the negative $\Delta^{26}Mg_{hemolymph\text{-}seawater}$ of specimen B3. In addition, Mg concentration in hemolymph appears 6–16% lower than surrounding seawater, reflecting Mg transport toward the soft tissues.

The isotopic composition of hemolymph can follow a different trend depending on whether Mg removal proceeds at or under chemical and isotopic equilibrium. In Fig. 9, unidirectional and equilibrium fractionation models are used to predict $\delta^{26}Mg$ of hemolymph as a function of Mg removal and under the condition of a constant fractionation factor. The unidirectional model implies that Mg is removed from a finite and well-mixed reactant reservoir (hemolymph) and becomes physically isolated in the product (no backward reaction). Under these conditions, Mg incorporation is unidirectional and $\delta^{26}Mg$ in the residual (hemolymph) can be described by the following approximation of the Rayleigh equation:

$$\delta^{26}Mg_{hemolymph} = \delta^{26}Mg_{seawater} + \Delta^{26}Mg_{softtissue\text{-}hemolymph} \times \ln f \quad (4)$$

where $\Delta^{26}Mg_{soft\ tissue\text{-}hemolymph} \approx 1000 \ln \alpha_{soft\ tissue\text{-}hemolymph}$ is the soft tissue-hemolymph isotope fractionation factor and f is the remaining Mg fraction in the hemolymph.

The equilibrium fractionation model includes two reservoirs (hemolymph and soft tissues) where isotope exchange proceeds under chemical equilibrium at any time of Mg removal (forward and backward reaction are identical) and where isotopic mass balance is preserved. The isotopic composition in the residual (hemolymph) material can be described by the following equation:

$$\delta^{26}Mg_{hemolymph} = \delta^{26}Mg_{seawater} - \Delta^{26}Mg_{softtissue\text{-}hemolymph} \times (1 - f) \quad (5)$$

For the two models, we have considered the same fractionation factor ($\Delta^{26}Mg_{soft\ tissue\text{-}hemolymph} \approx 1000 \ln \alpha_{soft\ tissue\text{-}hemolymph} = 0.56 \pm 0.29$‰, 2 sd) taken as the mean $\Delta^{26}Mg_{soft\ tissue\text{-}seawater}$ of soft tissues samples ($n = 6$). As shown in Fig. 9, $\delta^{26}Mg$ of hemolymph with the equilibrium model decreases during Mg incorporation in the soft tissues, but much less than with the unidirectional model.

To compare with the hemolymph samples, we estimated the remaining Mg fraction (f) in hemolymph relative to the surrounding seawater: it was 94% at Locmariaquer and ranged from 84% to 90% at Le Bono. For high values of f (>80%), the two models predict a similar deviation of −0.12‰ relative to seawater. As shown in Fig. 9, a good agreement can be found for four (out of five) hemolymph samples with our sample precision. For one sample (B3), $\delta^{26}Mg$ of −1.23‰ is still within the 95% confidence interval of the model, but unexplained variability is particularly high (−0.3‰), suggesting additional isotopic controls in the hemolymph.

4.4. Mg isotopes in the aragonitic bivalve shell

Following transfer through the soft parts, the final step of Mg incorporation takes place in EPF, where bivalve shell formation is biologically initiated (Weiner and Dove, 2003; Addadi et al., 2006; Jacob et al., 2008). Mg isotopic compositions reported for EPF and for aragonitic shell samples show the largest variability of the dataset, spanning more than 3‰. Averaged $\delta^{26}Mg$ of EPF remains close to hemolymph ($\Delta^{26}Mg_{EPF\text{-}Hemolymph} = 0.04 \pm 0.15$‰, $n = 5$) and to a lesser extent seawater ($\Delta^{26}Mg_{EPF\text{-}seawater} = -0.23 \pm 0.25$‰, 2 sd, $n = 5$). The close agreement found between hemolymph and EPF indicates that transport of Mg across

the OME to the calcifying fluid (from hemolymph to EPF) occurs without measurable isotopic fractionation, and that the hemolymph $\delta^{26}Mg$ signatures are tightly preserved in the EPFs. In individuals L1 and B1, $\Delta^{26}Mg_{EPF\text{-}seawater}$ are $-0.16‰$ and $-0.07‰$, respectively reflecting absence of fractionation from surrounding seawater. In contrast, in individuals B2, B3, and B4, $\Delta^{26}Mg_{EPF\text{-}seawater}$ of $-0.33‰$, $-0.37‰$, and $-0.20‰$, respectively support weak enrichments in the light isotope that derive essentially from the hemolymph compartment. As shown in Fig. 9, this may be tentatively explained by Mg incorporation into the soft tissues with unidirectional and equilibrium fractionation models. A good match can be found for three individuals (L1, B1 and B4) with our sample precision ($\pm 0.1‰$). For B2 and B3, measured $\delta^{26}Mg$ still lies within the 95% confidence interval of the two models, but unexplained fractionation of $\sim -0.2‰$ suggests additional isotopic controls.

Considering the aragonitic shell of the clam, measured Mg isotopic composition displays the largest variations and lightest Mg isotopic ratios of this study. Ranging from $-1.89 \pm 0.07‰$ to $-4.22 \pm 0.06‰$, shell $\delta^{26}Mg$ values exhibit systematic and variable fractionation towards light isotope compositions. As shown in Fig. 4, similar trends are observed in the two other aragonitic biocarbonates considered here: the bivalve *T. gigas* (SRM JCt-1) and the coral *Porites* sp. (SRM JCp-1). Shell $\delta^{26}Mg$ values are also consistent with the large array of negative $\delta^{26}Mg$ values reported for other marine calcifiers (Fig. 7) including the calcitic blue mussel *M. edulis* (Chang et al., 2004; Pogge von Strandmann, 2008; Hippler et al., 2009). As proposed in these studies, Mg isotope fractionation may include diverse levels of isotopic controls including abiotic and biologically-driven processes.

4.5. Mineralogical control of $\delta^{26}Mg$ in aragonite

The abiotic preferential incorporation of light Mg isotope in calcium carbonate is well documented for Low-Mg Calcite (LMC). LMC Speleothems were used to estimate a fractionation factor between mineral and drip water of $\Delta^{26}Mg_{LMC\text{-}drip\ water} = -2.7 \pm 0.10‰$ (Galy et al., 2002). A similar value is reported for another speleothem record ($\Delta^{26}Mg_{LMC\text{-}drip\ water} = -2.4‰$) and a slightly weaker fractionation is observed for abiogenic LMC precipitation experiments ($\Delta^{26}Mg_{LMC\text{-}solution} = -2.1‰$) (Immenhauser et al., 2010). Further insights by Mavromatis et al. (2012) point to a large variance (from $-3.16‰$ to $-1.88‰$) of the abiotic LMC Mg fractionation factor as a function of LMC precipitation rate, underlining the potential role of kinetic and growth rate factors.

The abiotic aragonite-seawater fractionation factor ($\Delta^{26}Mg_{aragonite\text{-}seawater}$) has recently been investigated via inorganic precipitation experiments ("free-drift") (Wang et al., 2013). $\Delta^{26}Mg_{aragonite\text{-}seawater}$ ($\approx 1000 \ln \alpha_{aragonite\text{-}seawater}$) appears weakly ($\sim 0.01‰/°C$) and inversely correlated with calcification temperature. At 15 °C, $\Delta_{26}Mg_{aragonite\text{-}seawater}$ can be estimated to $-1.18 \pm 0.28‰$ using the temperature equation of Wang et al. (2013). Considering the annual range of water temperature at the two sampling sites (7–21 °C), $\Delta^{26}Mg_{aragonite\text{-}seawater}$ is expected to vary by $0.15‰$ from $-1.27‰$ (7 °C) to $-1.12‰$ (21 °C). The $\Delta^{26}Mg_{aragonite\text{-}seawater}$ is therefore substantially smaller (~ 0.9–$2.1‰$) than $\Delta^{26}Mg_{LMC\text{-}seawater}$. Stronger ^{26}Mg enrichment in aragonite, where Mg sits in highly distorted sites with 9-fold coordination (Finch and Allison, 2007), possibly reflects shorter bond length and higher dissociation energy for Mg in aragonite than in calcite

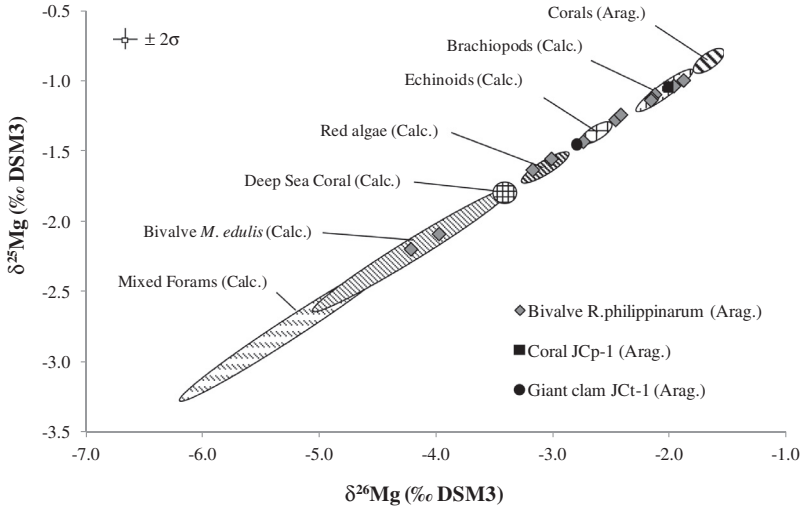

Fig. 7. Three-isotope plot ($\delta^{26}Mg$ vs. $\delta^{25}Mg$) of aragonitic shell of *R. philippinarum* (nacreous and prismatic components), reference materials JCp-1 (aragonitic coral) and JCt-1 (giant clam shell) and comparison with literature data available for corals (Chang et al., 2004), brachiopods, echinoids, red algae and bivalve *M. edulis* (Hippler et al., 2009), deep-sea coral and mixed foraminifers (Chang et al., 2004; Pogge von Strandmann, 2008). (Arag.) and (Calc.) refer to aragonitic and calcitic $CaCO_3$ polymorph, respectively.

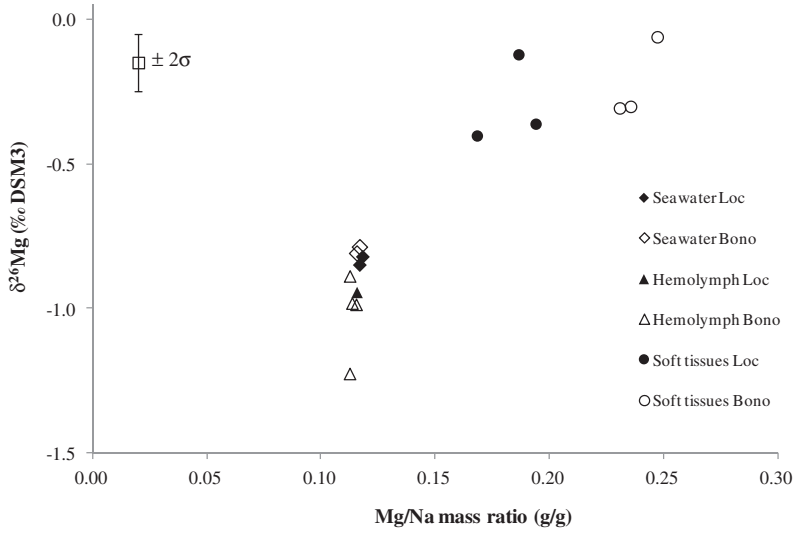

Fig. 8. Comparative plot of $\delta^{26}Mg$ (‰ vs. DSM3) vs. Mg/Na mass ratio (g/g) determined in the biological compartments (hemolymph and soft tissues) and the seawater samples collected at the two sampling sites (Locmariaquer and Le Bono). Uncertainties associated with $\delta^{26}Mg$ represent 2σ error (95% confidence interval).

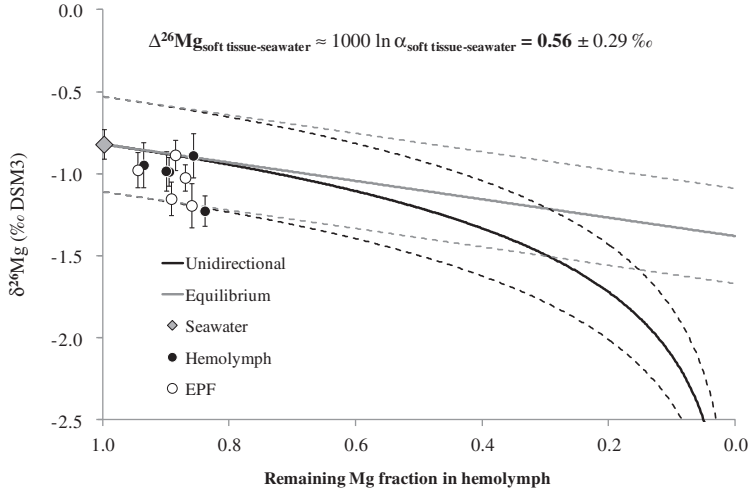

Fig. 9. Fractionation models for hemolymph as a function of Mg transfer in the soft tissues. Lines correspond to $\delta^{26}Mg$ of hemolymph evaluated with equilibrium (grey line) and unidirectional (dark line) models. The fractionation factor ($\Delta^{26}Mg_{\text{soft tissue-hemolymph}} \approx 1000 \ln \alpha_{\text{soft tissue-hemolymph}} = 0.56 \pm 0.29‰$) is deduced from $\delta^{26}Mg$ of bulk average soft tissues ($-0.26 \pm 0.09‰$, $n = 6$) and seawater ($-0.82 \pm 0.09‰$, $n = 4$). Also plotted: $\delta^{26}Mg$ determined in hemolymph and EPF samples vs. the remaining Mg fraction relative to surrounding seawater.

(Wang et al., 2013). The good agreement found between $\Delta^{26}Mg_{\text{aragonite-seawater}}$ and the theoretical equilibrium fractionation factor for magnesite (Rustad et al., 2010) suggests that fractionation in aragonite may represent isotope partitioning between a $MgCO_3$–H_2O cluster and Mg^{2+} aquocomplexes (Wang et al., 2013).

4.6. Physiological fractionation in the aragonitic bivalve shell

Mg-isotope fractionation factors measured in the shell of the manila clam ($\Delta^{26}Mg_{\text{shell-seawater}}$) can be compared to the inorganically precipitated aragonite ($\Delta^{26}Mg_{\text{aragonite-seawater}}$). As shown in Fig. 10, deviation from the inorganic precipitate is expressed as $\Delta^{26}Mg_{\text{Physiol}}$, corresponding to $\Delta^{26}Mg_{\text{shell-seawater}} - \Delta^{26}Mg_{\text{aragonite-seawater}}$. For the clam shell, $\Delta^{26}Mg_{\text{Physiol}}$ varies considerably, from close to zero ($\Delta^{26}Mg_{\text{Physiol}} = 0.03‰$, specimen L1, prismatic layer) to $-2.20‰$ (specimen B4, prismatic layer). This exceeds our analytical precision (~0.1‰) and also the 0.12‰ variability of $\Delta^{26}Mg_{\text{aragonite-seawater}}$ due to annual water temperature fluctuations (9–21 °C), and supports strong physiological isotopic effects registered in both the prismatic and the nacreous components. Negative $\Delta^{26}Mg_{\text{Physiol}}$ is consistent with light isotope enrichment in the biocarbonate relative to inorganic aragonite. Negative $\Delta^{26}Mg_{\text{Physiol}}$ is documented for other marine calcifiers, including some other bivalve species such as the aragonitic clam *T. gigas* (SRM JCt-1; $\Delta^{26}Mg_{\text{Physiol}} = -0.78‰$, this

study) and the calcitic blue mussel *M. edulis* ($\Delta^{26}Mg_{Physiol}$ range: 0.05‰ to −1.65‰) (Hippler et al., 2009), and also some mixed species of planktonic foraminifera ($\Delta^{26}Mg_{Physiol}$ range: −0.55‰ to −2.77‰) (Chang et al., 2004; Pogge von Strandmann, 2008; Wombacher et al., 2011). $\Delta^{26}Mg_{Physiol}$ can also take positive values, corresponding to enrichments in heavy isotope in the biomineral relative to the inorganically precipitated $CaCO_3$. This is seen in coccolith ooze ($\Delta^{26}Mg_{Physiol}$ range: 0.37–2.38‰), brachiopod ($\Delta^{26}Mg_{Physiol}$ range: 1.13–1.13‰) and echinoid tests ($\Delta^{26}Mg_{Physiol}$ range: 0.67–1.03‰), and to a lesser extent aragonitic corals and sclerosponges ($\Delta^{26}Mg_{Physiol}$ range: 0.19–0.52‰), and calcitic coralline red algae ($\Delta^{26}Mg_{Physiol}$ range: 0.18–0.45‰) (Hippler et al., 2009; Wombacher et al., 2011). Biominerals, where $\Delta^{26}Mg_{Physiol}$ appears negligible, are found in the aragonitic scaphopod ($\Delta^{26}Mg_{Physiol} = -0.05$‰), mixed species of calcitic warm water and deep sea corals ($\Delta^{26}Mg_{Physiol}$ range: −0.10 to 0.04‰), and mixed species of calcitic sclerosponge ($\Delta^{26}Mg_{Physiol}$ range: 0.04–0.25‰) (Wombacher et al., 2011), which suggests a calcifying process close to inorganic precipitation. Overall variation of $\Delta^{26}Mg_{Physiol}$ in biogenic carbonates spans more than 5‰ and shows either heavy or light isotope enrichments. This highlights the wide diversity of physiological isotopic controls that can affect Mg isotopes composition according to biomineralisation strategy.

4.6.1. Shell formation under close-to equilibrium conditions

Negligible values of $\Delta^{26}Mg_{Physiol}$ were found in four shell samples taken from the prismatic and the nacreous layers of specimen L1 collected at the coastal site Locmariaquer (mean $\Delta^{26}Mg_{Physiol} = -0.04 \pm 0.22$‰; 2 sd; $n = 4$), and in one prismatic sample of specimen B2 (1–2 mm growth increment) from Le Bono (with $\Delta^{26}Mg_{Physiol} = -0.17 \pm 0.13$‰). The absence of physiological controls suggests that the two shell components (prismatic and nacre) were precipitated under close-to conditions of inorganic equilibrium in terms of Mg isotopes. Such a fractionation pattern is consistent with passive Mg transport from the surrounding seawater to the calcifying fluid, followed by shell formation process similar to the inorganically-precipitated aragonite. This feature is reflected in the measured isotopic compositions of both the hemolymph and the EPF of specimen L1, which are the same, within

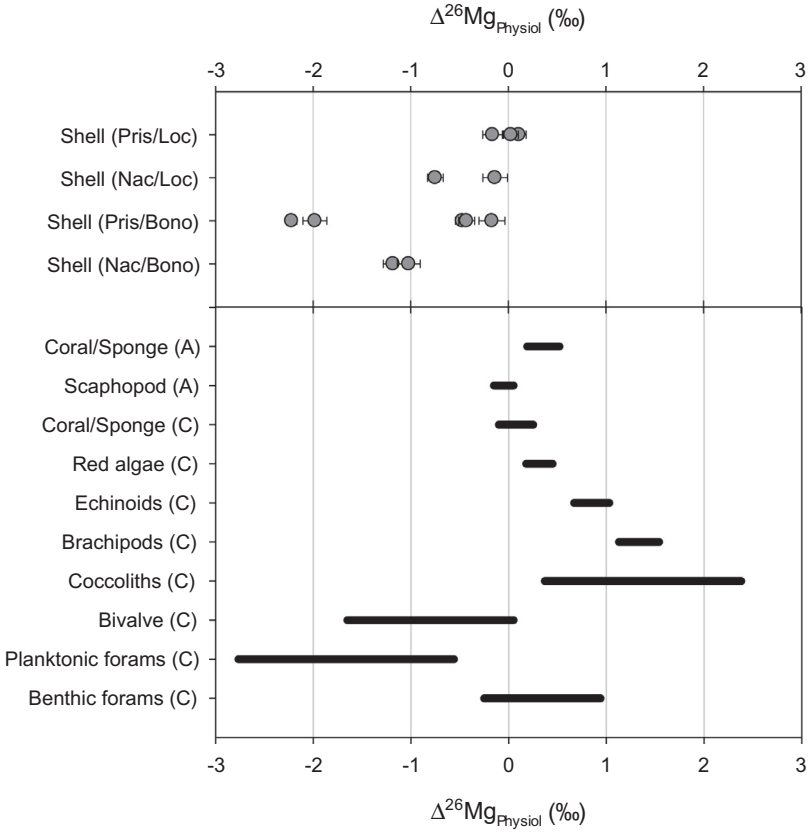

Fig. 10. $\Delta^{26}Mg_{Physiol}$ (‰) for the shell of the manila clam *R. philippinarum* (prismatic and nacreous layers) and comparison with published data for marine biogenic carbonates including scaphopods, bivalve *M. edulis*, echinoids, mixed foraminifera, and brachiopods (Chang et al., 2004; Pogge von Strandmann, 2008; Hippler et al., 2009; Wombacher et al., 2011). $\Delta^{26}Mg_{Physiol}$ refers to the difference in Mg-isotope fractionation factor between biocarbonate and seawater ($\Delta^{26}Mg_{biocarbonate\text{-}seawater}$), and inorganically-precipitated $CaCO_3$ and seawater ($\Delta^{26}Mg_{aragonite\text{-}seawater}$ or $\Delta^{26}Mg_{calcite\text{-}seawater}$). $\Delta^{26}Mg_{aragonite\text{-}seawater}$ ($\approx 1000 \ln \alpha_{aragonite\text{-}seawater}$) is estimated as -1.18 ± 0.28‰ at 15 °C using the temperature equation of Wang et al. (2013). $\Delta^{26}Mg_{calcite\text{-}seawater}$ is -2.7 ± 0.10‰ (Galy et al., 2002). (A) and (C) refer to aragonitic and calcitic biocarbonate, respectively.

analytical uncertainty, as the surrounding seawater $\Delta^{26}Mg_{hemolymph\text{-}seawater} = -0.16 \pm 0.13‰$ and $\Delta^{26}Mg_{EPF\text{-}seawater} = -0.13 \pm 0.15‰$. In addition, considering the temporal record provided by the consecutive samples taken from the prismatic layer of the left valve, the constant $\Delta^{26}Mg_{Physiol}$ of $0.11 \pm 0.07‰$ and of $0.03 \pm 0.08‰$ in the 0–1 and 1–2 mm growth increments (taken from the ventral margin and along maximum growth axis) respectively, tends to indicate that conditions close-to inorganic equilibrium have been maintained for approximately 40–100 days.

Bivalve shell formation similar to inorganically-formed aragonite remains relatively surprising given the facts that (1) Mg/Ca ratios in the clam shell (0.4–1.3 mmol/mol) are much lower than in inorganic precipitate (3.6–9.9 mmol/mol) (Gaetani and Cohen, 2006) suggesting a tight regulation of Mg content in the molluscan aragonite (Rosenheim et al., 2005a), and (2) Mg does not truly substitute for Ca in aragonite of bivalve shells (Foster et al., 2008; Takesue et al., 2008). However, evidence for physiological isotope effects can also be found in specimen L1, with $\Delta^{26}Mg_{Physiol} = -0.75‰$ in one nacre sample taken from the right valve. This physiological deviation was observed in only one valve, the nacre of the other valve staying close to the inorganic end-member ($\Delta^{26}Mg_{Physiol} = -0.14 \pm 0.15‰$). This may suggest that isotope fractionation is not homogeneously distributed within the organism and may be localized close to calcification site.

This hypothesis can be tested using Mg-isotope mass balance for specimen L1. Mass partitioning of Mg in the bivalve compartments was estimated from measured Mg concentrations combined with the weight of each component. Total dry weight of separated organs of soft tissues (mantle, adductor muscle, and remaining part) were not measured and were estimated using total shell weight and mean condition index (corresponding to soft tissues dry weight to shell dry weight ratio) of $8.8 \pm 1.9\%$ (1σ) estimated from an adult (two to 3 years old) clam population collected in the same geographical area and outside of the spawning period (Poulain et al., 2010). For hemolymph, we considered a total volume of 1 mL for this size manila clam (Ford and Paillard, 2007). Considering averaged Mg concentration in each compartment, Mg partitioning (molar fraction) in specimen L1 is as follows: 24% in the shell, 58% in the soft tissues, and 18% in hemolymph. EPF represented less than 2% of total Mg in the organism and was not taken into account in the isotopic mass balance calculation. Using averaged Mg isotopic signature for the soft tissues ($\delta^{26}Mg = -0.30 \pm 0.30‰$; 2 sd; $n = 3$), in hemolymph ($\delta^{26}Mg = -0.95 \pm 0.14‰$) and for the whole shell corrected for aragonite fractionation ($\delta^{26}Mg_{shell} = -1.00 \pm 0.67‰$, 2 sd, $n = 5$), isotopic mass balance had a $\delta^{26}Mg$ for the whole organism ($\delta^{26}Mg_w$) of $-0.57 \pm 0.74‰$ (2 sd). This is 0.25‰ heavier than the seawater source ($\delta^{26}Mg = -0.82‰$) and suggests that specimen L1 is not at steady state for Mg isotopes. The observed imbalance, although relatively uncertain (2 sd = 0.74‰), may indicate that there is no connection between Mg reservoirs. Hence, physiological effects evidenced in one nacre sample ($\Delta^{26}Mg_{Physiol} = -0.75‰$) of L1 may refer to a fractionation process restricted to the site of calcification and could be linked to the kinetics of aragonite precipitation.

4.6.2. Shell deposited under physiological influence

Physiological fractionation principally affects shell samples collected at the brackish water site (Le Bono), with strongly negative $\Delta^{26}Mg_{Physiol}$ of $-0.43‰$ to $-2.22‰$. As shown in Fig. 10, physiological effects systematically fractionate towards the light Mg isotope, and are recorded both in the prismatic ($\Delta^{26}Mg_{Physiol}$ range $-0.43‰$ to $-2.22‰$) and in the nacreous ($\Delta^{26}Mg_{Physiol}$ range $-1.02‰$ to $-1.18‰$) component of the shell. Prismatic samples taken at the ventral margin (0–1 mm growth increment) may provide a similar temporal record for a growth period of approximately 20–50 days at Le Bono site. Although growth rate can vary among individuals (Poulain et al., 2011), $\Delta^{26}Mg_{Physiol}$ registered in the 0–1 mm growth increments of specimens B1, B2, B3, and B4 (Table 2) varies from $-0.43‰$ in B3 to $-2.22‰$ in B4. Since individuals have experienced the same environmental conditions during the growth period, such a large variability suggests that $\Delta^{26}Mg_{Physiol}$ is poorly related to external parameters and is more probably controlled by biologically-mediated fractionation processes.

4.6.2.1. Mg partitioning between soft tissues and internal fluids. Negative $\Delta^{26}Mg_{Physiol}$ appears to be consistent with the biological fractionation identified between the intercellular fluid (hemolymph or EPF) and the solid organic component (soft tissues). As previously described, equilibrium and unidirectional models (Fig. 9) predict light isotope enrichments in the body fluid as a function of Mg removal, and agree with the trend of $\Delta^{26}Mg_{Physiol}$. In addition, mass balance calculation carried out for specimen B2 (the only specimen from Le Bono for which all compartments were considered) generated a different result compared to specimen L1. Following the same approach as for L1, Mg partitioning in B2 is 50% in the soft tissues, 25% in the hemolymph and 25% in the whole aragonitic shell. Combining the mean isotopic signature of the soft tissues ($-0.22 \pm 0.28‰$; 2 sd; $n = 3$), the hemolymph ($-0.99 \pm 0.09‰$), and the whole shell corrected for aragonite precipitation ($-1.89 \pm 2.56‰$; 2 sd; $n = 2$), we obtained a global $\delta^{26}Mg_w$ of $-0.81 \pm 2.56‰$ (2 sd). The whole shell signature was extrapolated from only two shell samples where $\Delta^{26}Mg_{Physiol}$ of $-0.17 \pm 0.13‰$ and of $-1.98 \pm 0.13‰$ is particularly variable. However, by contrast to specimen L1, $\delta^{26}Mg_w$ in specimen B2 appears closer to the seawater end-member, suggesting a steady state between the whole organism and the parent seawater. Physiological isotopic fractionation registered in the shell may be tentatively explained by Mg fractionation between the soft tissues and body fluids.

Here, we test this idea using the fractionation factor $\Delta^{26}Mg_{soft\ tissue\text{-}hemolymph} \approx 1000 \ln \alpha_{soft\ tissue\text{-}hemolymph} = 0.56 \pm 0.29‰$, and we calculate the remaining Mg fraction in the body fluid (f) which corresponds to the shell $\Delta^{26}Mg_{Physiol}$ value. For moderate $\Delta^{26}Mg_{Physiol}$ of $-0.43‰$ (B3, prismatic 0–1 mm), and $-0.47‰$ (B1, prismatic 0–1 mm), f is estimated to 47% and 43%, respectively with

the unidirectional model, and to 24% and 16%, respectively with the equilibrium model. For lightest physiological effects ($\Delta^{26}Mg_{Physiol} < -0.56‰$), only the unidirectional model can be applied. $\Delta^{26}Mg_{Physiol}$ of $-1.02‰$ (B3, nacre), $-1.18‰$ (B1, nacre), $-1.98‰$ (B2, prismatic 0–1 mm), and of $-2.22‰$ (B4, prismatic 0–1 mm) correspond to f of 16%, 12%, 3%, and 2%, respectively. It is interesting to note that the unidirectional model requires that Mg in the fluid becomes physically isolated when transferred to the soft tissues (no backward reaction) and furthermore that there is no additional supply of dissolved Mg to the fluid (finite reservoir). A similar fractionation model was tested to resolve the biological Mg-isotope fractionation observed in planktonic foraminifera *Globigerinoides ruber* with $\Delta^{26}Mg_{Physiol} = -1.5‰$ (Wombacher et al., 2011). Formation of foraminiferal calcite occurs in vacuoles of modified seawater from which Mg is actively removed in order to allow low-Mg calcite precipitation (Erez, 2003). A Rayleigh-type model (called here unidirectional model) used to account for Mg removal from the vacuole resulted in a fractionation factor $\Delta^{26}Mg_{foram} \approx 1000 \ln \alpha_{foram}$ of 0.48‰, similar to our value of 0.56‰. Wombacher et al. (2011) estimate that the remaining Mg fraction in the vacuole (f) is 2.3% at 10 °C, 4.5% at 20 °C, and 8.7% at 30 °C. This is in agreement with our f values, ranging from 2% to 16%. However, the temperature dependence of $\Delta^{26}Mg_{Physiol}$ in foraminiferal calcite calculated using Rayleigh-type removal appears inconsistent with the available *G. ruber* isotopic data (Wombacher et al., 2011). In our case, a substantial removal of Mg from the body fluid is required to match $\Delta^{26}Mg_{Physiol}$, and this is not supported by hemolymph and EPF data for which (1) f (relative to surrounding seawater) in the four individuals B1, B2, B3, and B4 remains higher than 84% suggesting a limited transfer to the soft tissues, and (2) measured fractionation in body fluids relative to seawater ($-0.41‰$ and $-0.37‰$ in hemolymph and EPF, respectively) is consistently weaker than expected by $\Delta^{26}Mg_{Physiol}$. For the EPF, the unexplained fractionation of $-1.52‰$ is particularly large, and suggests that in combination with Mg incorporation in the soft tissues other fractionation processes may control the isotopic composition of the shell.

4.6.2.2. Isotopic controls in calcifying fluid. Other controls may involve organic macromolecules contained in the EPF (e.g. proteins, polysaccharides, or glycoproteins) that supply a three dimensional template for bivalve shell formation (Addadi et al., 2006). As proposed by Wombacher et al. (2011), organic molecules can play a role in physiological effects recorded in *G. ruber* calcite ($\Delta^{26}Mg_{Physiol} = -1.5‰$) through complexation of dissolved Mg in vacuole. Using an equilibrium fractionation model and a remaining Mg fraction of 4.5% at 20 °C in the vacuole, a fractionation factor $\Delta^{26}Mg_{eq} \approx 1000 \ln \alpha_{eq} = 1.6‰$ is deduced and apparently matches the temperature dependency of $\Delta^{26}Mg_{Physiol}$ in planktonic foraminifera. Fractionation factor $\Delta^{26}Mg_{eq}$ of 1.6‰ for planktonic foraminifera is consistently higher than $\Delta^{26}Mg_{soft\ tissue\text{-}hemolymph} \approx 1000 \ln \alpha_{soft\ tissue\text{-}hemolymph} = 0.56 \pm 0.29‰$ determined here, but it reflects a similar enrichment in heavy isotope in the biologically-fixed Mg fraction. Using Eq. (5) and a fractionation factor $\Delta^{26}Mg_{eq}$ of 1.6‰ (Wombacher et al., 2011), we can account for physiological effects in the shell as light as $-1.6‰$ corresponding to a full Mg fixation onto organic molecules ($f = 0$). This could fit with five out of seven shell samples with $\Delta^{26}Mg_{Physiol}$ of $-0.47‰$ to $-1.18‰$. The calculated remaining Mg fractions in the EPF after organic fixation (f) are ~72% for B1 and B3 prismatic layers (0–1 mm growth increment), 53% for L1 nacreous layer (right valve), 36% for B3 nacreous layer, and 26% for B1 nacreous layer. The f values estimated using "equilibrium organic fixation model" are higher than the ones calculated with the soft tissue incorporation model, but they still disagree with EPF data which impose a f factor between 84% and 94%.

Regulation of Mg content in EPF may be supported by shell Mg/Ca ratios. As shown in Fig. 11, Mg/Ca ratios and $\Delta^{26}Mg_{Physiol}$ appear positively correlated in the two shell components. Deposited shell that is not or only weakly affected by physiological effects ($\Delta^{26}Mg_{Physiol} = 0‰$ down to $-0.5‰$) displays similar Mg/Ca ratios of 1.1 to 1.3 mmol/mol. For shell samples showing $\Delta^{26}Mg_{Physiol}$ lighter than ~$-0.5‰$, Mg/Ca ratios decrease to 0.9 to 0.4 mmol/mol. As previously observed in the aragonitic shell of *M. edulis* (Lorens and Bender, 1980), such a decrease in shell Mg/Ca ratios may be attributed to a decrease in Mg/Ca ratio of EPF. In addition, and despite the fact that the positive correlations are weakly constrained, the two shell components show different trends (Fig. 11). For similar Mg/Ca ratios (0.8–0.9 mmol/mol) registered in the two layers, $\Delta^{26}Mg_{Physiol}$ is significantly lower in the prismatic part (range: $-1.9‰$ to $-2.2‰$) compared to the nacre ($-0.7‰$). Considering that the nacre and the prismatic layer are precipitated from distinct extrapalleal fluids, located in the central part for the nacre and close to the shell margin for the prismatic layer, Mg isotopic compositions may be variable in the two isolated EPF even though Mg/Ca ratios stay comparable. However, information deduced from shell Mg/Ca ratios may not only refer to Mg/Ca ratio in EPF and must be carefully considered. Extensively studied as a potential temperature proxy, bivalve shell records of Mg/Ca ratios appear to be affected by diverse parameters including calcification temperature, growth dynamics, metabolic activity or even nutrient availability (e.g. Dodd and Crisp, 1982; Klein et al., 1996a; Vander Putten et al., 2000; Lazareth et al., 2003, 2007; Takesue and van Geen, 2004; Foster et al., 2008; Freitas et al., 2008). For the manila clam, potential factors influencing Mg/Ca ratios in the shell still have to be investigated in detail and are clearly relevant for further understanding.

4.6.2.3. Potential role of the shell organic matrix. In the prismatic shell of *Arctica islandica*, Mg is not substituted into aragonite but is hosted by a disordered phase such as organic components or nanoparticles of an inorganic phase (Foster et al., 2008). A similar finding was obtained for the aragonitic shell of *Corbula amurensis*, where a third of the Mg is removed with the shell organic matrix (Takesue

et al., 2008). If such a feature is also relevant for the shell of *R. philippinarum*, this may affect Mg fractionation during mineral formation through modification of the entrapment process at the mineral surface. Organic additive, such as a simple hydrophilic peptide with the same carboxyl-rich character as that of macromolecules isolated from sites of calcification, appears to decrease the desolvation barrier for Mg relative to Ca (Stephenson et al., 2008). Lowering the desolvation barrier for Mg would be expected to reduce the isotopic fractionation compared to inorganically-formed aragonite, but this is not supported by our data. Also, the organic framework of both prismatic and nacreous aragonites differs in organic content, amino acids, and sulfated compounds (Gotliv et al., 2003; Dauphin et al., 2005; Dalbeck et al., 2006). This difference could cause the lower slope of $\Delta^{26}Mg_{Physiol}$ vs. Mg/Ca ratio regression (Fig. 11) observed in the nacre ($\Delta^{26}Mg_{Physiol} = !\,1.09 \times Mg/Ca - 1.63$) compared to the prismatic shell ($\Delta^{26}Mg_{Physiol} = 4.28 \times Mg/Ca - 5.44$). Accordingly, the organic matrix of the nacreous layer could be associated with weaker Mg isotopic fractionation. However, a potential role for the shell organic matrix cannot easily be deciphered with our data, and needs further investigations to be fully understood. As an example, fractionation of Mg isotopes during hydrous magnesium carbonate precipitation appears to be identical in abiotic and in cyanobacteria-bearing experiments (Mavromatis et al., 2012), suggesting a limited influence of microbially-induced biomineralization.

Shell organic matrix is secreted by specialized epithelial cells of the OME and mass balance calculation reveals that soft tissues represent up to ~50% of total Mg mass of the organism. Therefore, soft tissues may provide an additional source of Mg to the shell in combination to dissolved Mg in the EPF. This may be possible if Mg stored in the soft tissues is incorporated into organic macromolecules during their secretion by the OME. However, the negative sign of $\Delta^{26}Mg_{Physiol}$ does not support direct incorporation of Mg from the solid organic compartment. Any mixing between the inorganically-precipitated aragonite $\delta^{26}Mg$ (−1.18‰ at 15 °C) and the heavier $\delta^{26}Mg$ of soft tissues (−0.06‰ to −0.40‰) would lead to positive $\Delta^{26}Mg_{Physiol}$ values. Interestingly, the same holds for dissolved Mg fixed onto organic macromolecules in the EPF. Given the fractionation factor $\Delta^{26}Mg_{eq} = 1.6‰$, heavy Mg isotope would be enriched (relative to parent fluid) in the fraction bound to organics. Therefore, if a significant amount of Mg stored in the soft tissues or complexed with organic molecules is incorporated into the shell, a subsequent fractionation step is required towards lighter values (at least lighter than $\delta^{26}Mg$ of inorganic aragonite −1.18‰ at 15 °C) to match $\Delta^{26}Mg_{Physiol}$. Such a fractionation step may occur in a similar way to Mg insertion into chlorophyll-a and -b molecules (Black et al., 2006, 2007). However, in order to confirm this idea it would be necessary to measure the Mg isotopic composition of the shell organic matrix and of the aragonite separately.

4.7. Influence of salinity regime on shell $\Delta^{26}Mg_{Physiol}$

One of the determining factors of physiological effects registered in the shell involves the collection site and the salinity regime experienced by the manila clam (Fig. 11). At the oceanic site, mean $\Delta^{26}Mg_{Physiol} = -0.16 \pm 0.13‰$ ($n = 5$) remains close to inorganically precipitated aragonite whereas at the brackish water site systematic and variable physiological effects ($\Delta^{26}Mg_{Physiol}$ ranging from −0.15‰ to −2.2‰; average: $-1.05 \pm 0.13‰$; $n = 7$) are observed. This compares to Mg isotopic data obtained for the calcitic bivalve *M. edulis* (Hippler et al., 2009), where $\Delta^{26}Mg_{Physiol}$ of *M. edulis* appear systematically lower at low salinity (mean $\Delta^{26}Mg_{Physiol} = -1.3 \pm 0.10‰$; $n = 6$; mean salinity: 28.5 psu) than at high salinity (mean $\Delta^{26}Mg_{Physiol} = -0.23‰ \pm 0.07‰$; $n = 4$; mean salinity: 29.3 psu). In that study, it was shown that Mg isotopic ratios were closely related to mean seasonal growth rates and that stronger physiological effects were encountered in fast-growing animals. Although a wide spectrum of factors influences shell growth, such a relationship gives further support for a biologically-driven fractionation of Mg isotope in the bivalves shell. In our study, growth dynamics of the prismatic and the nacreous shell was not investigated. However, detailed sclerochronological analysis was performed at Le bono on a similar subtidal adult clam population from May to October 2007 (Poulain et al., 2011). This study reveals that prismatic microgrowth increments are deposited with a tidal periodicity, which reflects a behavioral adaption of the valve closure at low tide in order to protect the clam from low salinities and/or to synchronize with food availability. Lunar daily growth increment widths ranging between 8 and 100 μm lunar day^{-1} exhibit a high inter-individual variability (Poulain et al., 2011). We observed a similar variability among individuals as evidenced by $\Delta^{26}Mg_{Physiol}$ of −0.43‰ to −2.20‰ in the 0–1 mm growth increment of individuals B1, B2, B3, and B4. This may indicate a potential link between physiological fractionation of Mg isotopes and the kinetics of shell precipitation. However, more detailed investigations are required to better assess this relationship.

The light $\Delta^{26}Mg_{Physiol}$ observed at the brackish water site may involve changes in seawater Mg concentrations according to tidal activity (maximum range: 5–53 mmol L^{-1}). As osmoconformers, decreases in seawater Mg concentrations are likely to be transferred to internal fluids (Neufeld and Wright, 1998; Shakhmatova et al., 2006). This could leave the hemolymph or the EFP more sensitive to isotopic fractionation when dissolved Mg is transferred to the soft tissues or adsorbed onto organic macromolecules in EPF. To confirm this hypothesis it would be necessary to measure body fluid isotopic compositions at higher frequency and over a full tidal cycle. However, variations in Mg concentrations should affect all specimens from the same site in a similar way, and this is not supported by the large inter-individual variability (from −0.45‰ to −2.2‰) registered in the 0–1 mm growth increment in B1, B2, B3 to B4 specimens. Other causes of physiological effects may involve the altered biological activity

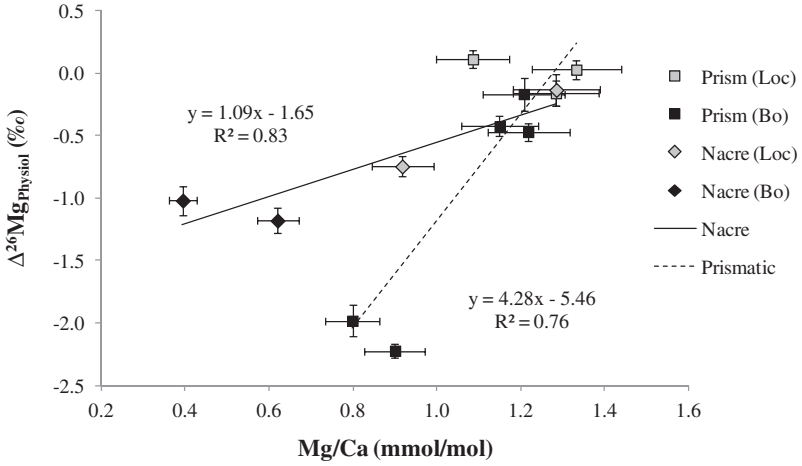

Fig. 11. Mg/Ca ratio plotted vs. $\Delta^{26}Mg_{Physiol}$ for shell samples of the Manila clam *R. philippinarum*. Regression lines obtained for the nacreous and prismatic components are indicated.

of the clam due to brackish water conditions. Salinity stress can affect several metabolic functions such as, for instance, osmotic regulation, protein synthesis, enzymatic activity, cell volume regulation, ATP synthesis and activation (Robert et al., 1993; Berger and Kharazova, 1997; Jordan and Deaton, 1999; Kim et al., 2001; Maguire and Cowan, 2002; Wolf and Cittadini, 2003; Kube et al., 2007). Mg being essential to most of these cellular processes, altered biological activity in salinity-stressed organisms could increase uptake fluxes of dissolved Mg from the hemolymph or the EPF. However, such a relationship between $\Delta^{26}Mg_{Physiol}$ and metabolic processes is difficult to assess with our data and more detailed studies are certainly required. One possible investigation could be to combine a detailed, time-resolved, profile of shell $\Delta^{26}Mg_{Physiol}$ with conventional chemical parameters and a detailed analysis of growth dynamics.

5. CONCLUSIONS

This study of the principal compartments involved in the biomineralisation process of a bivalve reveals that Mg isotopes are fractionated along their incorporation pathway from surrounding seawater to the shell. A first fractionation step takes place between the body fluids (hemolymph and EPF) and the solid organic samples. Fractionation factors $\Delta^{26}Mg_{soft\ tissue\text{-}seawater}$ of $0.42 \pm 0.12‰$ to $0.76 \pm 0.12‰$ were calculated and we propose that heavy isotope enrichments in the soft tissues are related to the transfer of Mg at the cell membrane interface. By contrast, hemolymph and EPF are on average isotopically identical to seawater suggesting (1) a predominant seawater origin for Mg in body fluids and (2) a relatively passive transfer route at the two successive epithelial barriers constituted by the IME and the OME. However, few EPF and hemolymph samples yield measurable fractionation with $\Delta^{26}Mg_{hemolymph\text{-}seawater} = -0.41 \pm 0.09‰$ or $\Delta^{26}Mg_{EPF\text{-}seawater} = -0.37 \pm 0.14‰$ which could be consistent with a limited Mg removal to the soft tissues combined with other unresolved fractionation processes.

The two components of the aragonitic shell (nacreous and prismatic) exhibit the lightest and the largest variations of the dataset, with $\delta^{26}Mg$ ranging from $-1.89 \pm 0.07‰$ to $-4.22 \pm 0.06‰$. Shell $\delta^{26}Mg$ are proposed to result from a combination of abiotic and biologically-driven fractionation processes. Abiotic controls include the mineral-fluid fractionation occurring during aragonitic precipitation, which has been estimated of $-1.18 \pm 0.28‰$ at 15 °C on the basis of the temperature calibration of Wang et al. (2013). Deviations from this inorganically-precipitated aragonite expressed as $\Delta^{26}Mg_{Physiol}$ vary from $0.03‰$ to $-2.20‰$ in the clam shell. These argue for variable levels of physiological isotopic effects affecting the two components of the aragonitic shell. Shell can be deposited either under close-to equilibrium conditions in terms of Mg isotopes ($\Delta^{26}Mg_{Physiol}$ close to zero), or under a strong physiological influence that could occur in self-contained spaces located close to calcification sites.

Physiological effects demonstrate a strong dependence on salinity regime. They preferentially affect individuals living in brackish water conditions. We propose that these effects could be related to the altered metabolic activity in salinity-stressed bivalves, which could involve protein synthesis, enzymatic activity, cell volume regulation, or ATP synthesis and activation. As outlined from earlier studies of Mg isotopes in biominerals and regarding the large physiological isotopic effects, Mg isotopic compositions in aragonitic bivalve shells offer limited if any potential as a proxy of temperature or even seawater Mg isotopic composition. On the other hand, sensitivity of Mg isotopic fractionation to salinity regime may pave the way for tracking changes in clam metabolism in estuarine environment.

ACKNOWLEDGMENTS

We thank J. Navez, L. Monin and N. Dakhani for laboratory assistance and for their help with ICP-AES and SF-ICP-MS analyses at the Royal Museum for Central Africa. Constructive comments by two anonymous reviewers, and by Josh West, with significant input from Marie-Laure Bagard are greatly appreciated

and helped improving the manuscript. We are also grateful to J. de Jong and N. Matielli (Free University of Brussels) for the management of the MC-ICP-MS lab and constant help in troubleshooting the instrument. This study was financially supported by the Belgian Federal Science Policy Office under the CALMARSII network (Contract SD/CS/02A of SPSDIII, Support Plan for Sustainable Development). Funding for the SF-ICP-MS instrument was provided by the Belgian Lotto, via the FWO-Flanders (contract G.0117.02N) and the Belgian Science Policy Office.

REFERENCES

Addadi L., Joester D., Nudelman F. and Weiner S. (2006) Mollusk shell formation: a source of new concepts for understanding biomineralization processes. *Chemistry* **12**, 980–987.

Adkins J. F., Boyle E. A., Curry W. B. and Lutringer A. (2003) Stable isotopes in deep-sea corals and a new mechanism for "vital effects". *Geochim. Cosmochim. Acta* **67**, 1129–1143.

Alvarez R. (1990) Recently developed NIST food related standard reference materials. *Fresen. J. Anal. Chem.* **338**, 466–468.

Berger V. J. and Kharazova A. D. (1997) Mechanisms of salinity adaptations in marine molluscs. *Hydrobiologia* **355**, 115–126.

Black J. R., Epstein E., Rains W. D., Yin Q.-z. and Casey W. H. (2008) Magnesium-isotope fractionation during plant growth. *Environ. Sci. Technol.* **42**, 7831–7836.

Black J. R., Yin Q.-z., Rustad J. R. and Casey W. H. (2007) Magnesium isotopic equilibrium in chlorophylls. *J. Am. Chem. Soc.* **129**, 8690–8691.

Black J. R., Yin Q.-z. and Casey W. H. (2006) An experimental study of magnesium-isotope fractionation in chlorophyll-a photosynthesis. *Geochim. Cosmochim. Acta* **70**, 4072–4079.

Bolou-Bi E. B., Poszwa A., Leyval C. and Vigier N. (2010) Experimental determination of magnesium isotope fractionation during higher plant growth. *Geochim. Cosmochim. Acta* **74**, 2523–2537.

Bolou-Bi E. B., Vigier N., Brenot A. and Poszwa A. (2009) Magnesium isotope compositions of natural reference materials. *Geostand. Geoanal. Res.* **33**, 95–109.

Brenot A., Cloquet C., Vigier N., Carignan J. and France-Lanord C. (2008) Magnesium isotope systematics of the lithologically varied Moselle river basin, France. *Geochim. Cosmochim. Acta* **72**, 5070–5089.

Buhl D., Immenhauser A., Smeulders G., Kabiri L. and Richter D. K. (2007) Time series δ^{26}Mg analysis in speleothem calcite: kinetic versus equilibrium fractionation, comparison with other proxies and implications for palaeoclimate research. *Chem. Geol.* **244**, 715–729.

Carré M., Bentaleb I., Bruguier O., Ordinola E., Barrett N. T. and Fontugne M. (2006) Calcification rate influence on trace element concentrations in aragonitic bivalve shells: evidences and mechanisms. *Geochim. Cosmochim. Acta* **70**, 4906–4920.

Chang V. T. C., Williams R. J. P., Makishima A., Belshawl N. S. and O'Nions R. K. (2004) Mg and Ca isotope fractionation during $CaCO_3$ biomineralisation. *Biochem. Biophys. Res. Commun.* **323**, 79–85.

Chang V. T. C., Makishima A., Belshaw N. S. and O'Nions R. K. (2003) Purification of Mg from low-Mg biogenic carbonates for isotope ratio determination using multiple collector ICP-MS. *J. Anal. At. Spectrom.* **18**, 296–301.

Crenshaw M. A. (1980) Mechanisms of shell formation and dissolution. In *Skeletal Growth of Aquatic Organisms: Biological Records of Environmental Change* (eds. D. C. Rhoads and R. A. Lutz). Plenum Publishing Corporation, New York, pp. 115–132.

Crenshaw M. A. (1972) The inorganic composition of molluscan extrapallial fluid. *Biol. Bull.* **143**, 506–512.

Dalbeck P., England J., Cusack M., Lee M. R. and Fallick A. E. (2006) Crystallography and chemistry of the calcium carbonate polymorph switch in *M. edulis* shells. *Eur. J. Mineral.* **18**, 601–609.

Dauphin Y., Cuif J. P., Salomé M. and Susini J. (2005) Speciation and distribution of sulfur in a mollusk shell as revealed by in situ maps using X-ray absorption near-edge structure (XANES) spectroscopy at the S K-edge. *Am. Mineral.* **90**, 1748–1758.

de Villiers S., Dickson J. A. D. and Ellam R. M. (2005) The composition of the continental river weathering flux deduced from seawater Mg isotopes. *Chem. Geol.* **216**, 133–142.

Dodd J. R. and Crisp E. L. (1982) Non-linear variation with salinity of Sr/Ca and Mg/Ca ratios in water and aragonitic bivalve shells and implications for paleosalinity studies. *Palaeogeogr. Palaeoclimatol. Palaeoecol.* **38**, 45–56.

Eble A. F. and Scro R. (1996) General anatomy. In *The Eastern Oyster Crassostrea virginica* (eds. V. S. Kennedy, R. I. E. Newell and A. F. Eble). Maryland Sea Grant Book, College Park, pp. 19–73.

Erez J. (2003) The source of ions for biomineralization in foraminifera and their Implications for paleoceanographic proxies. In *Biomineralization* (eds. P. M. Dove, J. J. De Yoreo and S. Weiner). Mineral Society of America, Washington, pp. 115–150.

Finch A. A. and Allison N. (2007) Coordination of Sr and Mg in calcite and aragonite. *Mineral. Mag.* **71**, 539–552.

Flatman P. W. (1984) Magnesium transport across cell membranes. *J. Membr. Biol.* **80**, 1–14.

Flye-Sainte-Marie J., Soudant P., Lambert C., Le Goïc N., Goncalvez M., Travers M.-A., Paillard C. and Jean F. (2009) Variability of the hemocyte parameters of *Ruditapes philippinarum* in the field during an annual cycle. *J. Exp. Mar. Biol. Ecol.* **377**, 1–11.

Ford S. E. and Paillard C. (2007) Repeated sampling of individual bivalve mollusks I: intraindividual variability and consequences for haemolymph constituents of the Manila clam, *Ruditapes philippinarum*. *Fish Shellfish Immunol.* **23**, 280–291.

Foster G. L., Pogge von Strandmann P. A. E. and Rae J. W. B. (2010) Boron and magnesium isotopic composition of seawater. *Geochem. Geophys. Geosyst.* **11**, Q08015.

Foster L. C., Finch A. A., Allison N., Andersson C. and Clarke L. J. (2008) Mg in aragonitic bivalve shells: seasonal variations and mode of incorporation in *Arctica islandica*. *Chem. Geol.* **254**, 113–119.

Freitas P. S., Clarke L. J., Kennedy H. A. and Richardson C. A. (2008) Inter- and intra-specimen variability masks reliable temperature control on shell Mg/Ca ratios in laboratory- and field-cultured *Mytilus edulis* and *Pecten maximus* (bivalvia). *Biogeosciences* **5**, 1245–1258.

Gaetani G. A. and Cohen A. L. (2006) Element partitioning during precipitation of aragonite from seawater: a framework for understanding paleoproxies. *Geochim. Cosmochim. Acta* **70**, 4617–4634.

Gagan M. K., Ayliffe L. K., Beck J. W., Cole J. E., Druffel E. R. M., Dunbar R. B. and Schrag D. P. (2000) New views of tropical paleoclimates from corals. *Quatern. Sci. Rev.* **19**, 45–64.

Galy A., Yoffe O., Janney P. E., Williams R. W., Cloquet C., Alard O., Halicz L., Wadhwa M., Hutcheon I. D., Ramon E. and Carignan J. (2003) Magnesium isotope heterogeneity of the isotopic standard SRM980 and new reference materials for magnesium-isotope-ratio measurements. *J. Anal. At. Spectrom.* **18**, 1352–1356.

Galy A., Bar-Matthews M., Halicz L. and O'Nions R. K. (2002) Mg isotopic composition of carbonate: insight from speleothem formation. *Earth Planet. Sci. Lett.* **201**, 105–115.

Galy A., Belshaw N. S., Halicz L. and O'Nions R. K. (2001) High-precision measurement of magnesium isotopes by multiple-collector inductively coupled plasma mass spectrometry. *Int. J. Mass Spectrom.* **208**, 89–98.

Geist J., Auerswald K. and Boom A. (2005) Stable carbon isotopes in freshwater mussel shells: environmental record or marker for metabolic activity? *Geochim. Cosmochim. Acta* **69**, 3545–3554.

Gillikin D. P., Lorrain A., Bouillon S., Willenz P. and Dehairs F. (2006) Stable carbon isotopic composition of *Mytilus edulis* shells: relation to metabolism, salinity, delta C-13(DIC) and phytoplankton. *Org. Geochem.* **37**, 1371–1382.

Gillikin D. P., Lorrain A., Navez J., Taylor J. W., Keppens E., Baeyens W. and Dehairs F. (2005) Strong biological controls on Sr/Ca ratios in aragonitic marine bivalve shells. *Geochem. Geophys. Geosyst.* **6**.

Gotliv B.-A., Addadi L. and Weiner S. (2003) Mollusk shell acidic proteins: in search of individual functions. *Chembiochem* **4**, 522–529.

Goulletquer P., Heral M., Deslous-Paoli J. M., Prou J., Garnier J., Razet D. and Boromthanarat W. (1989) Ecophysiologie et bilan énergétique de la palourde japonaise d'élevage *Ruditapes philippinarum*. *J. Exp. Mar. Biol. Ecol.* **132**, 85–108.

Grottoli A. G. and Eakin C. M. (2007) A review of modern coral $\delta^{18}O$ and $\delta^{14}C$ proxy records. *Earth Sci. Rev.* **81**, 67–91.

Henderson G. M. (2002) New oceanic proxies for paleoclimate. *Earth Planet. Sci. Lett.* **203**, 1–13.

Hippler D., Buhl D., Witbaard R., Richter D. K. and Immenhauser A. (2009) Towards a better understanding of magnesium-isotope ratios from marine skeletal carbonates. *Geochim. Cosmochim. Acta* **73**, 6134–6146.

Hippler D., Eisenhauer A. and Nägler T. F. (2006) Tropical Atlantic SST history inferred from Ca isotope thermometry over the last 140ka. *Geochim. Cosmochim. Acta* **70**, 90–100.

Hoenderop J. G. J. and Bindels R. J. M. (2008) Calciotropic and magnesiotropic TRP channels. *Physiology* **23**, 32–40.

Immenhauser A., Buhl D., Richter D., Niedermayr A., Riechelmann D., Dietzel M. and Schulte U. (2010) Magnesium-isotope fractionation during low-Mg calcite precipitation in a limestone cave – field study and experiments. *Geochim. Cosmochim. Acta* **74**, 4346–4364.

Immenhauser A., Nagler T. F., Steuber T. and Hippler D. (2005) A critical assessment of mollusk O-18/O-16, Mg/Ca, and Ca-44/Ca-40 ratios as proxies for Cretaceous seawater temperature seasonality. *Palaeogeogr. Palaeoclimatol. Palaeoecol.* **215**, 221–237.

Inoue M., Nohara M., Okai T., Suzuki A. and Kawahata H. (2004) Concentrations of trace elements in carbonate reference materials coral JCp-1 and giant clam JCt-1 by inductively coupled plasma-mass spectrometry. *Geostand. Geoanal. Res.* **28**, 417–429.

Jacob D. E., Soldati A. L., Wirth R., Huth J., Wehrmeister U. and Hofmeister W. (2008) Nanostructure, composition and mechanisms of bivalve shell growth. *Geochim. Cosmochim. Acta* **72**, 5401–5415.

Jordan P. J. and Deaton L. E. (1999) Osmotic regulation and salinity tolerance in the freshwater snail *Pomacea bridgesi* and the freshwater clam *Lampsilis teres*. *Comp. Biochem. Physiol. A Mol. Integr. Physiol.* **122**, 199–205.

Kim D. W. and Kang B. M. (2001) Enrichment of magnesium isotopes by 2′-aminomethyl-15-crown-5 bonded Merrifield peptide resin. *J. Radioanal. Nucl. Chem.* **250**, 291–294.

Kim D. W., Jeon B. K., Kang B. M., Lee N.-S., Ryu H.-i. and Lee Y.-i. (2003) Adsorption and isotope effects by ion exchange with 1-aza-12-crown-4 bonded Merrifield peptide resin. *J. Colloid Interface Sci.* **263**, 528–532.

Kim W. S., Huh H. T., Huh S. H. and Lee T. W. (2001) Effects of salinity on endogeneous rhythm of the Manila clam, *Ruditapes philippinarum* (Bivalvia: Veneridae). *Mar. Biol.* **2001**, 157–162.

Klein R. T., Lohmann K. C. and Thayer C. W. (1996a) Bivalve skeletons record of seas-surface temperature and $\delta^{18}O$ via Mg/Ca and $^{18}O/^{16}O$ ratios. *Geology* **24**, 415–418.

Klein R. T., Lohmann K. C. and Thayer C. W. (1996b) Sr/Ca and 13C/12C ratios in skeletal calcite of *Mytilus trossulus*: covariation with metabolic rate, salinity, and carbon isotopic composition of seawater. *Geochim. Cosmochim. Acta* **60**, 4207–4221.

Konrad M., Schlingmann K. P. and Gudermann T. (2004) Insights into the molecular nature of magnesium homeostasis. *Am. J. Physiol. Renal Physiol.* **286**, F599–F605.

Kube S., Sokolowski A., Jansen J. M. and Schiedek D. (2007) Seasonal variability of free amino acids in two marine bivalves, *Macoma balthica* and *Mytilus* spp., in relation to environmental and physiological factors. *Comp. Biochem. Physiol. A Mol. Integr. Physiol.* **147**, 1015–1027.

Lazareth C. E., Guzman N., Poitrasson F., Candaudap F. and Ortlieb L. (2007) Nyctemeral variations of magnesium intake in the calcitic layer of a Chilean mollusk shell (*Concholepas concholepas*, Gastropoda). *Geochim. Cosmochim. Acta* **71**, 5369–5383.

Lazareth C. E., vander Putten E., André L. and Dehairs F. (2003) High-resolution trace elements profiles in shells of the mangrove bivalve *Isognomon ephippium*: a record of environmental spatio-temporal variations? *Estuar. Coast. Shelf Sci.* **57**, 1103–1114.

Lord B. A. and DiBona D. R. (1976) Role of the septate junction in the regulation of paracellular transepithelial flow. *J. Cell Biol.* **71**, 967–972.

Lorens R. B. and Bender M. L. (1980) The impact of solution chemistry on *Mytilus edulis* calcite and aragonite. *Geochim. Cosmochim. Acta* **44**.

Maguire M. E. (2006) Magnesium transporters: properties, regulation and structure. *Front. Biosci.* **11**, 3149–3163.

Maguire M. E. and Cowan J. A. (2002) Magnesium chemistry and biochemistry. *Biometals* **15**, 203–210.

Mavromatis V., Pearce C. R., Shirokova L. S., Bundeleva I. A., Pokrovsky O. S., Benezeth P. and Oelkers E. H. (2012) Magnesium isotope fractionation during hydrous magnesium carbonate precipitation with and without cyanobacteria. *Geochim. Cosmochim. Acta* **76**, 161–174.

Mount A. S., Wheeler A. P., Paradkar R. P. and Snider D. (2004) Hemocyte-mediated shell mineralization in the eastern oyster. *Science* **304**, 297–300.

Müller M. N., Kısakürek B., Buhl D., Gutperlet R., Kolevica A., Riebesell U., Stoll H. and Eisenhauer A. (2011) Response of the coccolithophores *Emiliania huxleyi* and *Coccolithus braarudii* to changing seawater Mg^{2+} and Ca^{2+} concentrations: Mg/Ca, Sr/Ca ratios and $\delta^{44/40}Ca$, $\delta^{26/24}Mg$ of coccolith calcite. *Geochim. Cosmochim. Acta* **75**, 2088–2102.

Nadler M. J. S., Hermosura M. C., Inabe K., Perraud A.-L., Zhu Q., Stokes A. J., Kurosaki T., Kinet J.-P., Penner R., Scharenberg A. M. and Fleig A. (2001) LTRPC7 is a Mg ATP-regulated divalent cation channel required for cell viability. *Nature* **411**, 590–595.

Neufeld D. and Wright S. (1998) Effect of cyclical salinity changes on cell volume and function in *Geukensia demissa* gills. *J. Exp. Biol.* **201**, 1421–1431.

Neufeld D. S. and Wright S. H. (1996) Response of cell volume in *Mytilus* gill to acute salinity change. *J. Exp. Biol.* **199**, 473–484.

Nie Z. Q. (1991) The culture of marine bivalve mollusks in China. In *Estuarine and Marine Bivalve Mollusk Culture* (ed. W. Menzel). CRC Press, Boston, pp. 261–276.

Ourbak T., Corrège T., Le Cornec F., Charlier K. and Peypouquet J. P. (2006) A high-resolution investigation of temperature, salinity and upwelling activity proxies in corals. *Geochem. Geophys. Geosyst.* **7**.

Pearson N. J., Griffin W. L., Alard O. and O'Reilly S. Y. (2006) The isotopic composition of magnesium in mantle olivine: records of depletion and metasomatism. *Chem. Geol.* **226**, 115–133.

Pogge von Strandmann P. A. E. (2008) Precise magnesium isotope measurements in core top planktic and benthic foraminifera. *Geochem. Geophys. Geosyst.* **9**.

Pogge von Strandmann P. A. E., Burton K. W., James R. H., van Calsteren P., Gislason S. R. and Sigfússon B. (2008a) The influence of weathering processes on riverine magnesium isotopes in a basaltic terrain. *Earth Planet. Sci. Lett.* **276**, 187–197.

Pogge von Strandmann P. A. E., James R. H., van Calsteren P., Gíslason S. R. and Burton K. W. (2008b) Lithium, magnesium and uranium isotope behaviour in the estuarine environment of basaltic islands. *Earth Planet. Sci. Lett.* **274**, 462–471.

Poulain C., Lorrain A., Flye-Sainte-Marie J., Amice E., Morize E. and Paulet Y. M. (2011) An environmentally induced tidal periodicity of microgrowth increment formation in subtidal populations of the clam *Ruditapes philippinarum*. *J. Exp. Mar. Biol. Ecol.* **397**, 58–64.

Poulain C., Lorrain A., Mas R., Gillikin D. P., Dehairs F., Robert R. and Paulet Y. M. (2010) Experimental shift of diet and DIC stable carbon isotopes: influence on shell $\delta^{13}C$ values in the Manila clam *Ruditapes philippinarum*. *Chem. Geol.* **272**, 75–82.

Ra K. and Kitagawa H. (2007) Magnesium isotope analysis of different chlorophyll forms in marine phytoplankton using multi-collector ICP-MS. *J. Anal. At. Spectrom.* **22**, 817–821.

Ra K., Kitagawa H. and Shiraiwa Y. (2010) Mg isotopes and Mg/Ca values of coccoliths from cultured specimens of the species *Emiliania huxleyi* and *Gephyrocapsa oceanica*. *Mar. Micropaleontol.* **77**, 119–124.

Richardson C. A. (1987) Tidal Bands in the Shell of the Clam *Tapes philippinarum* (Adams & Reeve, 1850). *Proc. R. Soc. Lond. B Biol. Sci.* **230**, 367–387.

Robert R., Trut G. and Laborde J. L. (1993) Growth, reproduction and gross biochemical composition of the Manila clam *Ruditapes philippinarum* in the Bay of Arcachon, France. *Mar. Biol.* **116**, 291–299.

Romani A. M. P. and Maguire M. E. (2002) Hormonal regulation of Mg^{2+} transport and homeostasis in eukaryotic cells. *Biometals* **15**, 271–283.

Rosenheim B. E., Swart P. K. and Thorrold S. R. (2005a) Minor and trace elements in sclerosponge *Ceratoporella nicholsoni*: biogenic aragonite near the inorganic endmember? *Palaeogeogr. Palaeoclimatol. Palaeoecol.* **228**, 109–129.

Rosenheim B. E., Swart P. K., Thorrold S. R., Eisenhauer A. and Willenz P. (2005b) Salinity change in the subtropical Atlantic: secular increase and teleconnections to the North Atlantic Oscillation. *Geophys. Res. Lett.* **32**.

Rustad J. R., Casey W. H., Yin Q.-Z., Bylaska E. J., Felmy A. R., Bogatko S. A., Jackson V. E. and Dixon D. A. (2010) Isotopic fractionation of $Mg^{2+}_{(aq)}$, $Ca^{2+}_{(aq)}$, and $Fe^{2+}_{(aq)}$ with carbonate minerals. *Geochim. Cosmochim. Acta* **74**, 6301–6323.

Schöne B. R. and Gillikin D. P. (2013) Unraveling environmental histories from skeletal diaries – advances in sclerochronology. *Palaeogeogr. Palaeoclimatol. Palaeoecol.* **373**, 1–5.

Shakhmatova E., Berger V. and Natochin Y. (2006) Cations in molluscan tissues at sharply different hemolymph osmolality. *Biol. Bull.* **33**, 269–275.

Sinclair D. J. and Risk M. J. (2006) A numerical model of trace-element coprecipitation in a physicochemical calcification system: application to coral biomineralization and trace-element 'vital effects'. *Geochim. Cosmochim. Acta* **70**, 3855–3868.

Stephenson A. E., DeYoreo J. J., Wu L., Wu K. J., Hoyer J. and Dove P. M. (2008) Peptides enhance magnesium signature in calcite: insights into origins of vital effects. *Science* **322**, 724–727.

Takesue R. K. and van Geen A. (2004) Mg/Ca, Sr/Ca, and stable isotopes in modern and Holocene *Protothaca staminea* shells from a northern California coastal upwelling region. *Geochim. Cosmochim. Acta* **68**, 3845–3861.

Takesue R. K., Bacon C. R. and Thompson J. K. (2008) Influences of organic matter and calcification rate on trace elements in aragonitic estuarine bivalve shells. *Geochim. Cosmochim. Acta* **72**, 5431–5445.

Teng F. Z., Wadhwa M. and Helz R. T. (2007) Investigation of magnesium isotope fractionation during basalt differentiation: implications for a chondritic composition of the terrestrial mantle. *Earth Planet. Sci. Lett.* **261**, 84–92.

Tipper E. T., Galy A. and Bickle M. J. (2008a) Calcium and magnesium isotope systematics in rivers draining the Himalaya-Tibetan-Plateau region: lithological or fractionation control? *Geochim. Cosmochim. Acta* **72**, 1057–1075.

Tipper E. T., Louvat P., Capmas F., Galy A. and Gaillardet J. (2008b) Accuracy of stable Mg and Ca isotope data obtained by MC-ICP-MS using the standard addition method. *Chem. Geol.* **257**, 65–75.

Tipper E. T., Galy A., Gaillardet J., Bickle M. J., Elderfield H. and Carder E. A. (2006) The magnesium isotope budget of the modern ocean: constraints from riverine magnesium isotope ratios. *Earth Planet. Sci. Lett.* **250**, 241–253.

Turekian K. K. (1968) *Oceans*. Prentice-Hall.

Urey H. C., Lowenstam H. A., Epstein S. and McKinney C. R. (1951) Measurements of paleotemperatures and temperatures of the Upper Cretaceous of England, Denmark, and the southeastern United States. *Geol. Soc. Am. Bull.* **62**, 399.

Van der Wijst J., Hoenderop J. G. J. and Bindels R. J. M. (2009) Epithelial Mg^{2+} channel TRPM6: insight into the molecular regulation. *Magnes. Res.* **22**, 127–132.

Vander Putten E., Dehairs F., Keppens E. and Baeyens W. (2000) High resolution distribution of trace elements in the calcite shell layer of modern *Mytilus edulis*: environmental and biological controls. *Geochim. Cosmochim. Acta* **64**, 997–1011.

Walker C. J. and Willows R. D. (1997) Mechanism and regulation of Mg-chelatase. *Biochem. J.* **327**, 321–333.

Wanamaker A. D. J., Kreutz K. J., Schöne B. R., Pettigrew N., Borns H. W., Introne D. S., Belknap D., Maasch K. A. and Feindel S. (2008) Coupled North Atlantic slope water forcing on Gulf of Maine temperatures over the past millennium. *Clim. Dyn.* **31**, 183–194.

Wang Z., Hu P., Gaetani G., Liu C., Saenger C., Cohen A. and Hart S. (2013) Experimental calibration of Mg isotope fractionation between aragonite and seawater. *Geochim. Cosmochim. Acta* **102**, 113–123.

Warren M. A., Kucharski L. M., Veenstra A., Shi L., Grulich P. F. and Maguire M. E. (2004) The CorA Mg^{2+} transporter is a homotetramer. *J. Bacteriol.* **186**, 4605–4612.

Weiner S. and Dove P. M. (2003) An overview of biomineralization processes and the problem of the vital effect. *Rev. Mineral. Geochem.* **54**, 1–29.

Wheeler A. P. (1992) Mechanisms of molluscan shell formation. In *Calcification in Biological Systems* (ed. E. Bonucci). CRC Press, Boca Raton, pp. 179–216.

Wolf F. I. and Cittadini A. (2003) Chemistry and biochemistry of magnesium. *Mol. Aspects Med.* **24**, 3–9.

Wolf F. I., Torsello A., Fasanella S. and Cittadini A. (2003) Cell physiology of magnesium. *Mol. Aspects Med.* **24**, 11–26.

Wombacher F., Eisenhauer A., Böhm F., Gussone N., Regenberg M., Dullo W. C. and Rüggeberg A. (2011) Magnesium stable isotope fractionation in marine biogenic calcite and aragonite. *Geochim. Cosmochim. Acta* **75**, 5797–5818.

Wombacher F., Eisenhauer A., Heuser A. and Weyer S. (2009) Separation of Mg, Ca and Fe from geological reference materials for stable isotope ratio analyses by MC-ICP-MS and double-spike TIMS. *J. Anal. At. Spectrom.* **24**, 627–636.

Yago M. D., Mañas M. and Singh J. (2000) Intracellular magnesium: transport and regulation in epithelial secretory cells. *Front. Biosci.* **5**, d602–d618.

Yoshimura T., Tanimizu M., Inoue M., Suzuki A., Iwasaki N. and Kawahata H. (2011) Mg isotope fractionation in biogenic carbonates of deep-sea coral, benthic foraminifera, and hermatypic coral. *Anal. Bioanal. Chem.* **401**, 2755–2769.

Young E. D. and Galy A. (2004) The isotope geochemistry and cosmochemistry of magnesium. *Rev. Mineral. Geochem.* **55**, 197–230.

Young E. D., Galy A. and Nagahara H. (2002) Kinetic and equilibrium mass-dependent isotope fractionation laws in nature and their geochemical and cosmochemical significance. *Geochim. Cosmochim. Acta* **66**, 1095–1104.

Associate editor: Derek Vance